1
2

Loss of Nrf1 rather than Nrf2 leads to inflammatory accumulation of lipids and reactive oxygen species (ROS) in human hepatoma cells, which is alleviated by 2-bromopalmitate

3   Rongzhen Deng[1,2,3,†], Ze Zheng[1,†], Shaofan Hu[1,2,3], Meng Wang[1], Jing Feng[1], Peter Mattjus[4], Zhengwen Zhang[5] and Yiguo Zhang[2,3*]

4   [1]Bioengineering College and Graduate School, Chongqing University, No. 174 Shazheng Street, Shapingba District, Chongqing 400044, China

5   [2]Chongqing University Jiangjin Hospital, School of Medicine, Chongqing University, No. 725 Jiangzhou Avenue, Dingshan Street, Jiangjin District, Chongqing
6   402260, China

7   [3]The Laboratory of Cell Biochemistry and Topogenetic Regulation, College of Bioengineering and Faculty of Medical Sciences, Chongqing University, No. 174
8   Shazheng Street, Shapingba District, Chongqing 400044, China

9   [4]Department of biochemistry, Faculty of Science and Engineering, Åbo Akademi University, Artillerigatan 6A, III, BioCity, FI-20520, Turku, Finland

10 [5]Laboratory of Neuroscience, institute of Cognitive Neuroscience and School of Pharmacy, University College London, 29-39 Brunswick Square, London WC1N
11   1AX, England, United Kingdom

12 * Correspondence should be addressed to: yiguozhang@cqu.edu.cn, or eaglezhang64@gmail.com

13 † Contributed equally to this work.

14 **Abstract**:

15 Since Nrf1 and Nrf2 are essential for regulating the lipid metabolism pathways, their dysregulation has thus been
16 shown to be critically involved in the non-controllable inflammatory transformation into cancer. Herein, we have
17 explored the molecular mechanisms underlying their distinct regulation of lipid metabolism, by comparatively
18 analyzing the changes in those lipid metabolism-related genes in $Nrf1\alpha^{-/-}$ and/or $Nrf2^{-/-}$ cell lines relative to wild-type
19 controls. The results revealed that loss of Nrf1α leads to lipid metabolism disorders. That is, its lipid synthesis pathway
20 was up-regulated by the JNK-Nrf2-AP1 signaling, while its lipid decomposition pathway was down-regulated by the
21 nuclear receptor PPAR-PGC1 signaling, thereby resulting in severe accumulation of lipids as deposited in lipid droplets.
22 By contrast, knockout of Nrf2 gave rise to decreases in lipid synthesis and uptake capacity. These demonstrate that
23 Nrf1 and Nrf2 contribute to significant differences in the cellular lipid metabolism profiles and relevant pathological
24 responses. Further experimental evidence unraveled that lipid deposition in $Nrf1\alpha^{-/-}$ cells resulted from CD36
25 up-regulation by activating the PI3K-AKT-mTOR pathway, leading to abnormal activation of the inflammatory response.
26 This was also accompanied by a series of adverse consequences, e.g., accumulation of reactive oxygen species (ROS) in
27 $Nrf1\alpha^{-/-}$ cells. Interestingly, treatment of $Nrf1\alpha^{-/-}$ cells with 2-bromopalmitate (2BP) enabled the yield of lipid droplets
28 to be strikingly alleviated, as accompanied by substantial abolishment of CD36 and critical inflammatory cytokines.
29 Such $Nrf1\alpha^{-/-}$ led inflammatory accumulation of lipids, as well as ROS, was significantly ameliorated by 2BP. Overall,
30 this study provides a potential strategy for cancer prevention and treatment by precision targeting of Nrf1, Nrf2 alone
31 or both.

32 **Key words**: Nrf1; Nrf2; lipid metabolism; lipid droplets; JNK; AP1; mTOR; CD36; IL-6; ROS; 2-bromopalmitate (2BP)

1. Introduction

34   Lipids are essential for energy storage, assembles into macromolecular structures as biomembranes, and function in
35 cell growth, proliferation, differentiation, and movement. Many types of lipids act as biological signaling molecules and
36 thus exert diverse functionality in energy metabolism and cell homeostasis [1-3]. However, abnormal lipid metabolism
37 is connected to a variety of diseases. For instance, obesity caused by over-nutrition, nonalcoholic steatohepatitis
38 (NASH), and type 2 diabetes, are all related to the imbalance in the lipid metabolism status [4]. Importantly, the
39 development of hepatocellular carcinoma (HCC) is also linked to lipid disorders, such as NASH [5]. This is due to the
40 fact that most cancer cells had been shown to have a higher rate of *de novo* lipid synthesis, leading to an obvious
41 increase in newly synthesized fatty acids, glycerophospholipids and cholesterol. These serve as raw materials to meet
42 the increasing requirements of cancer cells for their malignant growth and proliferation. In addition, the up-regulated
43 catabolism of lipids by β-oxidation in the mitochondria can also provide additional energy, as required by those cancer

44 cells [6].

45   In almost all living organisms, lipids are stored in the form of triglycerides and cholesterol-esters in lipid droplets

46 (LDs). This hydrophobic organelle with a surrounding phospholipid monolayer membrane, can mobilize fatty acids

47 during specific life processes [7]. Since the liver is the main metabolic organ of lipids in vertebrates, lipids play a vital

48 role in the physiological homeostasis of the liver and related pathological processes of many liver diseases. The

49 liver-specific mouse knockout of *Nrf1* (also called *Nfe2l1*, encoding a 'living fossil-like' conserved membrane-bound

50 transcription factor of the cap'n'collar (CNC) basic-region leucine zipper (bZIP) family [8]) leads to spontaneous

51 development of NASH and its ensuing malignant transformation into hepatoma [9]. Such hepatocyte-specific loss of

52 *Nrf1* caused up-regulation of the cytochrome p450 family *CYP4A* and *CYP1A1* genes, hepatic microsomal lipid

53 peroxidation to be substantially increased, and then fatty acids and cystine/cysteine contents to be aberrantly

54 accumulated, as consequently followed by severe steatosis, apoptosis, necrosis, inflammation, and fibrosis, eventually

55 worsening and developing into liver cancer [10, 11]. During this pathogenesis, significant activation of two lipid

56 metabolism-related genes, *Lipin1* and *PGC-1β* was observed in the murine liver-specific $Nrf1^{-/-}$ cells, implying that Nrf1

57 negatively regulates these two genes by directly binding to the putative antioxidant response elements (AREs) located

58 in their promoter regions [12].

59   Nrf2 (also encoded by *Nfe2l2*, a soluble transcription factor of the CNC-bZIP family) has been shown to regulate

60 lipid metabolism by mediating the expression of several lipid metabolism-related genes, such as those encoding ACLY,

61 ACC1 and ELOVL6 [13, 14]. It was found by Huang *et al* [15] that $Nrf2^{-/-}$ mice manifested with a loss of their liver

62 weight at six months of age, together with a marked decrease of the triacylglycerol contents in the liver. These changes

63 in the liver of $Nrf2^{-/-}$ mice had led to the up-regulation of lipogenic genes including *PPARγ, FASN, SCD1* and *SREBP1*,

64 albeit they were proved to serve direct target genes of Nrf2 [15]. Adipose-specific ablation of *Nrf2* in mice can also

65 cause a transient delay of high-fat diet-induced obesity by altering glucose, lipid, and energy metabolism in such mice

66 [16]. Taken together, these findings demonstrate that Nrf2 acts as an important regulator of lipid metabolism. However,

67 how Nrf1 and Nrf2 differentially govern (and reciprocally regulate) the lipid metabolism process, in particular liver

68 cancer cells, is still poorly understood to date.

69   In this study, we focus on the lipid synthesis and catabolism, as well as the mechanism related to lipid deposition,

70 by conducting various experiments to determine the yields of lipid droplets in $Nrf1\alpha^{-/-}$ cells (in which the full-length

71 Nrf1 of 742 aa was deleted by its gene editing) and its changes in the lipid metabolism gene expression, as compared

72 to the data obtained from in $Nrf2^{-/-}$ cells. The results unveiled that Nrf1 and Nrf2 have performed their respective

73 regulatory functions in the lipid metabolism of hepatoma cells through distinct molecular mechanisms. Further

74 experiments also revealed that both CNC-bZIP factors are differentially involved in putative cytoprotection against

75 inflammatory response to abnormal lipid metabolism caused by $Nrf1\alpha^{-/-}$ and/or $Nrf2^{-/-}$. Interestingly, lipid deposition

76 and related inflammation responses are significantly reduced by a palmitic acid analogue, 2-bromopalmitate (2BP).

77 Collectively, this study provides a novel potential strategy for the prevention and treatment of NASH and hepatoma by

78 precision targeting of Nrf1, Nrf2 alone or both.

79 **2. Materials and Methods**

80 *2.1 Cell lines and culture*

81   The human HepG2 cells (i.e., $Nrf1/2^{+/+}$) were obtained from the American Type Culture Collection (ATCC, Manassas,

82 VA, USA). $Nrf1\alpha^{-/-}$ and $Nrf2^{-/-}$ cell lines were established on the base of HepG2 cells in our laboratory by Qiu *et al* [17].

83 Besides, Nrf1α-restored cell line was created by employing lentivirus technology to allow for stable expression of Nrf1

84 α proteins and also identified to be true. The fidelity was further confirmed by its authentication profiling and STR

85 (short tandem repeat) typing map (Shanghai Biowing Applied Biotechnology Co., Ltd). All these cell lines were cultured

86 at 37℃ with 5% CO2 in Dulbecco's modified Eagle's medium (DMEM) containing 25 mmol/L glucose, 10% (v/v) fetal

87 bovine serum (FBS), 100 units/mL penicillin-streptomycin, before subsequent experiments were performed.

88 **2.2 Real-time quantitative PCR analysis**

89 The total RNAs were extracted from experimental cells when they reached 80% confluency using an RNA extraction

90 kit (TIANGEN, Beijing, China) and then reversely transcribed into single-stranded cDNAs by a Reverse-Transcription Kit

91 (Promega, USA). In parallel experiments, the cell lines that were subjected to different treatments with specific

92 inhibitors or siRNAs (to interfere with its cognate target gene expression) were subjected to similar RNA extraction

93 procedure. The mRNA expression levels of each target gene were determined by real-time quantitative PCR (i.e.,

94 RT-qPCR) with each of those indicated pairs of their forward and reverse primers (listed in Table 1).

95 **Table 1.** All oligonucleotides and antibodies that were used in this study.

96 (i) The primer pairs that were used for RT-qPCR analysis.

Gene Name	Forward Primers (5' to 3')	Reverse Primers (5' to 3')
β-actin	GCGGCTACAGCTTCACCAC	GCCATCTCTTGCTCGAAGTCCA
Nrf1	CCCCTGCTCTTCAAAACAACC	ATCTTGCCACTGCTGTTCC
Nrf2	AGTCCAGAAGCCAAACTGACA	ATGCTGCTGAAGGAATCCTCA
FASN	ATTCGACCTTTCTCAGAACCAC	AAGAACGCATCCAGTAGGAC
SCD1	ATGCTAATTCAATGCCGCAAC	CTTCCCCAGCAGAGACCAC
ACCα	CTCAGAGGCGAGAAACTCCA	CATCAATCGCTCTACCCAGT
SREBP1	GCCATCGACTACATTCGCTTT	GCACGTCTGTGTTCCCTCC
HO1	CAGTGCCACCAAGTTCAAGCA	CTTGGCCTCTTCTATCACCCT
JUN	ATGGAAACGACCTTCTATGACGA	CGTTGCTGGACTGGATTATCA
NQO1	ATTCCTTAGCCTGGATTTCCT	GCACGAATACAGTCGATTCCC
GCLM	ACGAGAATCGCTTGAACCT	AGTTTTCCCAGGCAAATCACA
GCLC	CCCGATATGACTCAATAGACAGC	ATGATCAATGCCTTCCTGCAAC
CD36	TACAGATGCAGCCTCATTTCCAC	ACAGCATAGATTGACCTGCAAA
IL-6	CAAATGTAGCATGGGCACCT	AACATAAGTTCTGTGCCCAGT
IL-1β	CCTGCCCACAGACCTTCCAG	AAGCCTCGTTATCCCATGTGT
NFκB1	CGTCAGAAGCTCATGCCCAA	GCCACTACCAAACATGCCTCC
NFκB2	CCTGAAGCCAGTCATCTCCC	GCACCTTGTCACAAAGCAGA
TNFα	CCCTCAACCTCTTCTGGCTCA	GCCACACATTCCTGAATCCCA

97 (ii) Oligonucleotides sequences of siRNA.

Name	Forward Primers (5' to 3')	Reverse Primers (5' to 3')
siNrf2	GUAAGAAGCCAGAUGUUAAdTdT	UUAACAUCUGGCUUCUUACdTdT
siJUN	GCAUGGACCUAACAUUCGAdTdT	UCGAAUGUUAGGUCCAUGCdTdT

98 (iii) The key antibodies used in this work.

Antibodies	Identifier	Source
Nrf1	N/A	Zhang laboratory [18]
Nrf2	ab62352	Abcam
ACCα	D155300	Sangon Biotech
FASN	D262701	Sangon Biotech
SCD1	D162163	Sangon Biotech
SREBP1	14088-1-AP	Proteintech
ATGL	ab109251	Abcam
PPARα	D161086	Sangon Biotech
PPARγ	ab272718	Abcam
PPARδ	ab178866	Abcam
PGC-1α	D262041	Sangon Biotech
PGC-1β	D162042	Sangon Biotech
JNK	ab208035	Abcam
p-JNK	ab124956	Abcam
JUN	10024-2-AP	Proteintech
FOS	ab134122	Abcam
HO1	ab68477	Abcam
AKT1	ab32505	Abcam
p-AKT	ab38449	Abcam
p-mTOR^{2448}	ab109268	Abcam
p-mTOR^{2481}	ab137133	Abcam
PI3K	ab245781	Abcam
CD36	ab133625	Abcam
COX2	ab62331	Abcam
IL-6	ab233706	Abcam
NFκB	ab32360	Abcam
p-NFκB	ab140751	Abcam
β-actin	TA-09	ZSGB-BIO

2.3 Small interfering RNAs and kinase-specific inhibitors

To determine the effect of a given gene on the downstream signaling, the JNK function inhibitor SP600125 (Selleck, Shanghai, China), the PI3K inhibitor NVP-BKM120 (Cayman Chemical, USA), and the mTOR inhibitor RAPA (rapamycin, Sigma, USA) were used here. Two pairs of small-interfering RNAs (siRNAs, with their oligonucleotide sequences listed in Table 1) were designed for specifically targeting Nrf2 or JUN (i.e., siNrf2 or siJUN), in order to interfere with their mRNA expression levels (Tsingke, Beijing, China).

2.4 Western blotting analysis of key proteins

All experimental cells were subjected to extraction of total proteins in a lysis buffer containing a protease inhibitor cOmplete Tablets EASYpack or phosphatase inhibitor PhosSTOP EASYpack (each tablet per 15 mL buffer, Roche, Basel,

4

108 Switzerland). The proteins in cell lysates were denatured at 100℃ for 10 min, followed by sonication, and then diluted
109 in 3×loading buffer (187.5 mmol/L Tris-HCl, pH 6.8, 6% SDS, 30% Glycerol, 150 mmol/L DTT, and 0.3% Bromphenol Blue)
110 at 100℃ for 5 min. Thereafter, equal amounts of cell lysates were separated by SDS-PAGE gels (8-12% polyacrylamide)
111 and the specific proteins visualized by Western blotting with antibodies listed in Table 1.

112 *2.5 Determination of intracellular triglyceride contents*

113 All the relevant experimental cells were subjected to determination of the triglyceride (TG) contents, as
114 conducted according to the manufacture's instruction using a TG-enzymatic assay kit (APPLYGEN, Beijing, China). After
115 discarding the medium and rinsing the cells with PBS for three times, 170 μL of a working solution (prepared by mixing
116 reagent R1 with reagent R2 at the ratio of 4:1 on ice) was added into every well of 96-wells plate. And then this plate
117 was incubated at room temperature for 15 min, before quantitative absorbance was measured at 570 nm by using
118 spectrophotometer (Thermo Scientific, Shanghai, China).

119 *2.6 Oil Red O-staining of lipid droplets in cells*

120 After the cells reached 70% of confluency, they were subjected to different treatments with different
121 concentrations of oleic acid (OA, Solarbio, Beijing, China) or 2-bromopalmitate (2BP, Sigma, USA). Then, the cells were
122 fixed in a tissue fixative buffer containing 4% paraformaldehyde (Boster Biological Technology, Wuhan, China) for 30
123 min, followed by lipid droplet staining for 30 min in a solution containing 3 g/L of oil red O (Sangon Biotech, Shanghai,
124 China). Finally, the stained cells were rinsed three times with 60% of isopropyl alcohol (Kelong, Chengdu, China), and
125 the red lipid droplets were visualized and photographed by microscopically imaging analysis.

126 *2.7 Assays of ARE-driven luciferase reporter gene activity*

127 Equal numbers (2.0×10^5) of experimental cells ($Nrf1/2^{+/+}$) were seeded into each well of the 12-well plates. After
128 reaching 80% confluence, the cells were co-transfected using a Lipofectamine 3000 mixture with each of lipid
129 catabolism related *ARE*-driven luciferase reporters (constructed by inserting each of the *ARE*-battery sequences of lipid
130 catabolism related gene into the pGL3-Promoter vector) or non-*ARE* plasmids (as a background control), together with
131 an expression construct for Nrf1 or empty pcDNA3.1 vector. In the same time, the *Renilla* expression by pRL-TK
132 plasmid served as an internal control for transfection efficiency. Approximately 24 hours after transfection, the
133 reporter activity was measured by using the dual-luciferase reporter assay kit (Promega, USA). The resulting data were
134 calculated as fold changes (mean ± S.D., n = 9), relative to the basal activity (at a given value of 1.0) obtained from the
135 transfection of cells with an empty pcDNA3.1 and each of *ARE*-driven reporter genes. These *ARE*-core sequences are
136 shown in Table 2.

137 **Table 2**. The *ARE*-drive reporter sequences from the lipid catabolism related gene promoters.

Gene Name	Sequence Number	Sequence
ATGL	1	TTGAGACGGAGTCTTGCTCTGTCACCCAGGCTGGAGCAC
	2	TTGAGAAGAAGTCATGCTCTGTCACCTGGCCAGGCTGGA
	3	CTGGAGTGCAGTGGTGCGATCTCAGCTCACTGCAACCTC
	4	CCTCCCACCCCAACCTGAGAAAGCCTCTCGTTTGGGGGT
PGC-1α	1	TATTGTAAGTTTGAAGCCAGGTCAGTCAGCATTATTTGG
	2	AGTTTGATGTAGCATTGACTTAGCTTAACTACAGCAACC

	3	TGTCCCCGGCAGCCGGCGGAGTCAGCGCGCCCACGTGAC
	4	TGCGCCTCCATCCCGGCTCGCTCATTATCTCGCCCTCTC
	1	AAAAAGGGACCTGAGACAGCATTGTCACCACATAAATGG
PPARα	2	ATGTGCAAGAGAAGGTGAGGTTGCCGTGTGCCAGTGGGA
	3	CGGAGCTGGGGCGTCGCCGACTCAGAAGGTGCTTTCCGA
	1	GGGTCCGGGGCTGAGGCAGGGTCATGGTCCGGCAGGACC
PPARγ	2	CGCGTGCGTCCGTCCTGAGGCCGCGCGGCACCCCTGCTG
	3	TTCCCTTTCCTTAGGTGAGTTGGCTCACTCTCATTGCAT

2.8 ChIP-sequencing analysis

The CHIP-sequencing data for Nrf1 (called Nfe2l1) binding to the promoter region of interested target genes in HepG2 cells obtained from the Encode database (https://www.encodeproject.org) with the project number ENCSR543SBE), were analyzed herein.

2.9. Analysis of cellular reactive oxygen species (ROS) by flow cytometry

Equal numbers (3.0×10^5) of experimental cells were seeded into each well of the 6-well plates. At 70% confluency, they were transferred to a fresh medium with or without 2BP for 24 h and then prepared according to the manufacture's instruction for the ROS assay kit (Beyotime, Shanghai, China). The cells were collected and suspended in diluted DCFH-DA (which was diluted with serum-free medium at 1:1000 to achieve a final concentration of 10 μM), before being incubated for 20 min at 37℃ in a cell incubator. Mix upside down every 3-5 min so that the probe is allowed for a full contact with the cells, before they were then washed three times with a serum-free medium. Thereafter, the intracellular ROS levels were determined by flow cytometry (at Ex/Em = 488/525nm). The resulting data were analyzed by the FlowJo 7.6.1 software, as described previously [19]. Similar experiments were obtained by using a Mito-Tracker Red CMXRos ROS test kit (Beyotime, Shanghai, China).

2.10. Statistical analysis

Significant differences for the obtained data were statistically determined using the Student's *t*-test or Multiple Analysis of Variations (MANOVA). The data are shown herein as a fold change (mean ± S.D.), each of which represents at least three independent experiments that were each performed in triplicates.

3. Results

3.1. Knockout of Nrf1α in hepatoma cells leads to lipid deposition while knockout of Nrf2 leads to lipid reduction.

A striking feature in the pathology of NASH is lipid deposition, which is also a hall-mark of liver cancer development in murine $Nrf1^{-/-}$-disordered lipid metabolism [10, 11]. Herein, wild-type HepG2 cells ($Nrf1/2^{+/+}$) and two derived cell lines ($Nrf1α^{-/-}$ and $Nrf2^{-/-}$) were employed in the following experiments to investigate distinct functionality of Nrf1 and Nrf2 in human intracellular lipid metabolism. These cell lines were further validated by Western blotting and real-time qPCR analyses of Nrf1 and Nrf2 (Fig. 1, A & B). The results were fully consistent with our previous data [17, 19] when comparing the wild-type $Nrf1/2^{+/+}$ controls to $Nrf1α^{-/-}$ cells. Such $Nrf1α^{-/-}$ cells exhibited no expression of Nrf1α-derived proteins, but other shorter isoforms of Nrf1ß and Nrf1γ were unaltered (Fig.1A, *upper panel*). By contrast, Nrf2 protein amounts (Fig.1A, *middle panel*) and its basal mRNA levels (Fig. 2B) were significantly increased in $Nrf1α^{-/-}$ cells. Nrf1α-derived proteins were slightly enhanced in $Nrf2^{-/-}$ cells lacking its two major proteins (Fig. 1A,

167   *right lane*), but this was accompanied by a modest decrease in the basal mRNA expression of Nrf1 (Fig. 1, A & B).

168   These indicate putative inter-regulation of Nrf1α and Nrf2 that could be executed at distinct levels.

169   After 24-h treatment of distinct cell lines with oleic acid (OA) at different concentrations (0, 50, 100 μmol/L), the

170   lipid droplets were examined by oil red O staining. The data is shown in Fig. 1C. When compared with wild-type

171    $Nrf1/2^{+/+}$ controls, much more and larger lipid droplets were found in $Nrf1\alpha^{-/-}$ cells, whereas small lipid droplets were

172   in $Nrf2^{-/-}$ cells. There was a significant difference in the visualization of lipid droplets after OA treatment of these three

173   cell lines with incrementing concentrations of OA from 50 to 100 μmol/L (Fig. 1C). Such an OA-increased trend of lipid

174   droplets was seen in $Nrf1\alpha^{-/-}$ cells that were significantly higher than that of $Nrf1/2^{+/+}$ controls, while $Nrf2^{-/-}$ cells also

175   manifested a reduced visualization of lipid droplets. These unraveled that loss of $Nrf1\alpha$ led to an aberrant

176   accumulation of lipids, whereas similar lipid deposition appeared to be alleviated by inactivation of Nrf2. This finding

177   was also further evidenced by an intracellular triglyceride (TG) enzymatic detection assay of those same cell lines that

178   had been treated with 100 μmol/L OA (Fig. 1D). Their distinct TG contents (in lipid droplets) were also visualized by oil

179   red O staining, as shown in Fig. 1E. These distinct results demonstrated that loss of Nrf1α enables the lipid deposition

180   to be augmented in $Nrf1\alpha^{-/-}$ hepatoma cells, but a similar lipid-accumulating phenomenon was not observed in $Nrf2^{-/-}$

181   cells. The latter further implies that its lipid synthesis and/or uptake may have been suppressed by $Nrf2$-specific

182   knockout of its transactivation domain (i.e., $Nrf2^{-/-\Delta TA}$) rather than its DNA-binding domain as described previously

183   [20].

184   ***3.2 Loss of Nrf1α or Nrf2 causes different effects on the expression of genes responsible for lipid metabolism.***

185   It has been shown that genes governing the *de novo* lipid synthesis were expressed in cancer cells to a

186   considerably greater extent than their equivalents in normal cells [21]. Therefore, a few of key rate-limiting enzymes

187   (e.g., FASN, ACCα, SCD1) of *de novo* lipid synthesis and regulated transcriptional factor SREBP1 (sterol regulatory

188   element-binding protein 1) were examined next. As anticipated, our results revealed that the loss of $Nrf1\alpha^{-/-}$ caused a

189   substantial increase in the protein expression of FASN (fatty acid synthase), ACCα (acetyl-CoA carboxylase alpha), SCD1

190   (stearoyl-Coenzyme A desaturase 1) and SREBP1 when compared to their counterparts in wild-type $Nrf1/2^{+/+}$ cells (Fig.

191   2A). Similar augmented expression levels of mRNA were also observed in $Nrf1\alpha^{-/-}$ cells when analyzed using real-time

192   qPCR (Fig. 2B). Conversely, the lentivirus-mediated recovery of Nrf1α in $Nrf1\alpha^{-/-}$ cells (i.e., Nrf1α-restored cell line, as

193   illustrated in Figs. S1 & S2A) enabled to cause a substantial decrease in the protein expression of FASN, ACCα, SCD1

194   and SREBP1 when compared to $Nrf1\alpha^{-/-}$ cells (Fig. S2B). These indicate that aberrant expression of lipid

195   synthesis-related genes is caused by the absence of $Nrf1\alpha$. By striking contrast, $Nrf2^{-/-}$ cells gave rise to

196   down-regulated expression levels of the same genes to greater or fewer degrees (Fig. 2, A & B).

197   Further examinations of $Nrf1\alpha^{-/-}$ cells revealed a considerably lower expression level of adipose triglyceride lipase

198   (ATGL, also called PNPLA2, which is the catalytic rate-limiting enzyme in the first step of TG hydrolysis during oxidation

199   catabolic mobilization [22], Fig. 2C & D). A small decrease in the expression of ATGL was also determined in $Nrf2^{-/-}$ cells

200   as compared to wild-type cells (Fig. 2C & D). Further experimental analysis of the nuclear receptor-types (i.e., PPARα, γ,

201   δ) of transcription factors governing oxidative degradation of fatty acids [23] and their interacting transcriptional

202   co-activators (i.e., PGC-1α, β) [24] was carried out. The results showed that all the examined proliferator-activated

203   receptors (PPARα, γ, δ) and PPARγ co-activators (PGC-1α, -1β) were significantly down-regulated in $Nrf1\alpha^{-/-}$ cells

204   (retaining a hyper-active Nrf2), and thus were roughly unaffected in $Nrf2^{-/-}$ cells, but except for down-expressed

205   PPARα only (Fig. 2, C & D). Conversely, ATGL, PGC-1α and PPARα were significantly up-regulated in Nrf1α-restored cells,

206 as compared with $Nrf1\alpha^{-/-}$ cells (Fig. S2C). Such differential expression patterns of PPARα, γ and δ regulated by Nrf1

207 and/or Nrf2 implies a selectivity to mediate distinct downstream genes, and thus it is inferable that PPARγ and PPARδ

208 are the main downstream of Nrf1α, whereas PPARα is not. Conversely, upon loss of Nrf1α, the former two factors will

209 be down-regulated, while the latter one has no significant changes. Taken altogether, these collective data

210 demonstrate that abnormal deposition of lipids in $Nrf1\alpha^{-/-}$ cells result from up-regulation of lipid anabolism, along

211 with substantial down-regulation of lipid catabolism-controlled genes, but the opposite effects seem to be obtained in

212 $Nrf2^{-/-}$ cells.

213   Next, the differential expression profiles of lipid synthesis- and catabolism-related genes between $Nrf1\alpha$- and

214 $Nrf2$-deficient cell lines were further explored. The results showed a markedly increased presence of phosphorylated

215 JNK and its cognate target JUN in $Nrf1\alpha^{-/-}$ cells (with a hyper-active Nrf2) (Fig. 2E, $e2$ to $e4$), although the total protein

216 level of JUK was slightly down-regulated (Fig. 2E, $e1$) when compared to wild-type controls. However, Nrf1α-restored

217 cells only manifested a modest decreased expression level of JUN (Fig. S2C). By contrast, all those examined protein

218 levels were strikingly diminished upon inactivation of $Nrf2^{-/-}$ (Fig. 2E). Such similarly-altered expression trends of Nrf2,

219 p-JUNK and JUN seem to presage a comparable pattern to those of the lipogenic genes, thereby providing a new clue

220 for the further study of their relevant gene regulation.

221 ***3.3 The JNK-Nrf2-AP1 signaling is required for up-regulation of lipogenic and HO-1 genes in Nrf1α-deficient cells.***

222   As shown in Fig. 3A ($a1$ to $a8$), treatment of $Nrf1\alpha^{-/-}$ cells with a JNK-specific inhibitor SP600125 (to block the

223 activity of phosphorylated JNK) caused substantial down-regulation of all seven other examined proteins, including

224 Nrf2, JUN (a direct substrate of JNK), HO-1, FASN, ACCα, SCD1 and SREBP1. Notably, the lipid synthesis-related ACCα

225 and SCD1 displayed a profound inhibitory trend similar to those of JUN and Nrf2, but SREBP1 appeared to be only

226 partially inhibited by SP600125. This implies that the JUK signaling to Nrf2 and/or AP1 is involved in the aberrant

227 lipogenesis of $Nrf1\alpha^{-/-}$ cells. The treated cells still retained a remnant fraction of JUN and Nrf2, but their direct

228 downstream HO-1 expression was almost completely abolished by SP600125 (Fig. 3A, *cf. a4 with a2 and a3*),

229 implicating an integrative effect of both factors on HO-1.

230   Further experiments revealed that silencing of Nrf2 by its specific *siNrf2* (to interfere with its mRNA expression in

231 $Nrf1\alpha^{-/-}$ cells) also led to obvious down-regulation of AP1 (i.e., a heterodimer of JUN and FOS), HO-1 (a direct co-target

232 of Nrf2 and AP1), and those lipogenic enzymes FASN, ACCα and SCD1 (Fig. 3B, *b1 to b6*). Next, the real-time qPCR

233 analysis showed that knockdown of *Nrf2* by its *siNrf2* caused significantly reduced expression of *JUN, FASN, ACCα* and

234 *SCD1* (Fig. 3C). This indicates a predominant requirement for Nrf2 in regulating AP1 and the key enzymes in lipid

235 synthesis, besides its cognate target genes *HO-1, NQO1, GCLC* and *GCLM* (Fig. 3C). However, SREBP1 appeared to be

236 roughly unaffected by the silencing of Nrf2 (Fig. 3, B & C).

237   Interestingly, *siJUN* knockdown of AP1 activity in $Nrf1\alpha^{-/-}$ cells led to marked decreases in the expression of FASN,

238 ACCα and SCD1 at their protein and mRNA levels (Fig. 3, D & E). However, SREBP1 was almost unaltered by silencing of

239 JUN by siJUN (as shown in this study), although it was shown to regulate activation of specific genes (such as LGALS3)

240 in response to cholesterol loading and hence plays an important role in reprogramming lipid metabolism [25]. Rather,

241 it should also be noted that SREBP1 may not have synergistic regulation with triglycerides-related lipogenic enzymes in

242 this process, albeit lipid droplets are composed of neutral lipids (triglycerides and cholesterol) [26]. Further

243 examination of $Nrf1\alpha^{-/-}$ cells by transfecting expression constructs for JUN alone or plus FOS revealed that such forced

244 expression of AP1 led to up-regulation of SCD1, but FASN was unaffected (Fig. 3F, *c.f. f5 with f3*). Intriguingly, only a

245 marginal increase of ACCα was caused by overexpression of JUN alone, but conversely, a substantial decrease of this
246 enzyme was dictated by co-expression of JUN and FOS (Fig. 3F, *f4*). Such dual opposite regulation of ACCα by JUN alone
247 or plus FOS may be determined by a putative functional heterodimer of JUN with another bZIP partner competing
248 together with the AP1 factor, depending on distinct experimental settings.

249 **3.4 Nrf1α$^{-/-}$ cell-autonomous induction of the PI3K-AKT-mTOR signaling leads to abnormal hyper-expression of**
250 **CD36.**

251 An important nutritional metabolism mechanism sets into action by the signaling of the PI3K
252 (phosphatidylinositol 3-kinase) to its downstream AKT (also called protein kinase B) and mTOR (mechanistic target of
253 rapamycin kinase) [27]. Upon activation of mTOR by stimulation of nutritional signals, it enables for up-regulation of
254 CD36 (as a key regulator of fatty acid uptake and its transport [28]). As anticipated, a significant increase in the basal
255 constitutive expression of CD36 was found in *Nrf1α$^{-/-}$* cells, when compared with wild-type controls (Fig. 4A, *a6*). Such
256 aberrant hyper-expression of CD36 was accompanied by dominant cell-autonomous activation of PI3K^{P110Δ} and AKT, as
257 well as of phosphorylated AKT and mTOR at distinct sites (Fig. 4A, *a1 to a5*). In addition, the loss of Nrf1α in *Nrf1α$^{-/-}$*
258 cells led to the basally-augmented expression of a general inflammatory marker COX2 (cyclooxygenase 2, as shown in
259 Fig. 4A, *a7*); this key enzyme, also called prostaglandin-G/H synthase (PTGS2), is involved in arachidonic acid
260 metabolism. Conversely, Nrf1α-Restored cells gave rise to significant suppression of COX2, CD36, PI3K^{p110Δ},
261 phosphorylated AKT and mTOR, when compared with their counterparts in *Nrf1α$^{-/-}$* cells (Fig. S2, D & E).

262 To determine whether *Nrf1α$^{-/-}$* cell-autonomous activation of the PI3K-AKT-mTOR signaling is required for
263 up-regulation of CD36 by its deficiency, a PI3K-specific inhibitor NVP-BKM120 (Fig. 4B) and another mTOR-specific
264 inhibitor rapamycin (RAPA, Fig. 4C) were used for treatment of *Nrf1α$^{-/-}$* and *Nrf1/2$^{+/+}$* cell lines, respectively. As
265 expected, the results revealed that two phosphorylated protein levels of mTOR were substantially diminished by
266 NVP-BKM120 and RAPA in their treated cell lines (Figs. 4B, *b1 & b2* and 4C, *c1 & c2*). The basal expression levels of
267 COX2 and CD36 were also almost abrogated by NVP-BKM120 and RAPA (Figs. 4B, *b7 & b8* and 4C, *c8 & c9*). However,
268 no or less effects of both inhibitors on all other examined proteins (e.g., JNK, Nrf1, Nrf2 and HO-1) were determined
269 (Figs. 4B, *b3 to b6* and 4C, *c3 to c7*). This demonstrates that loss of Nrf1α enables to cause a non-controllable
270 activation status of CD36, as well as COX2, primarily by the PI3K-AKT-mTOR signaling pathway.

271 Since such up-regulation of CD36 can also assist the Toll-like receptor 4 (TLR4) with synergistic activation of the
272 inflammatory factor NFκB and cytokines IL-6, IL-1β and TNFα [29], next we determine whether their changed
273 expression levels in *Nrf1α$^{-/-}$* cells have relevance to the hyper-expression of CD36. The results unveiled that the
274 dramatic activation of CD36 by loss of Nrf1α was accompanied by varying enhancements of NFκB, IL-6, IL-1ß, and TNFα
275 at their protein and/or mRNA expression levels in *Nrf1α$^{-/-}$* cells, when compared with those equivalents of *Nrf1/2$^{+/+}$*
276 cells (Fig. 4, D & E). In addition, the recovery of Nrf1α in *Nrf1α$^{-/-}$* cells led to apparent decreases in the expression of
277 NFκB and IL-6 (Fig. S2E). Overall, it is postulated that *Nrf1α$^{-/-}$*-disordered lipid metabolism may be attributable to
278 aberrant activation of CD36, along with a concomitant inflammatory response.

279 **3.5 The inflammatory accumulation of lipids and ROS in Nrf1α$^{-/-}$ cells is alleviated by 2-bromopalmitate.**
280 As shown schematically in Fig. 5A, 2BP is a palmitic acid analogue with one bromine (Br) atom at the β-C position,
281 allowing for dramatic improvement of its stability that is more than that of the prototypic palmitate. The
282 physicochemical property of 2BP enables this palmitic acid analogue to block biological processes in which palmitic

283 acids should have participated. For example, 2BP was employed as a natural ligand of PPARδ receptor in fatty acid
284 oxidation [30]. Here we found that triglyceride (TG) accumulation in $Nrf1\alpha^{-/-}$ cells was significantly inhibited by 2BP
285 (Fig. 5B). Similar treatments with 2BP caused almost abolishment of basal CD36 expression in both $Nrf1\alpha^{-/-}$ and
286 $Nrf1/2^{+/+}$ cell lines (Fig. 5C), and also enabled for substantial suppression of lipid droplets in $Nrf1\alpha^{-/-}$ cells to
287 considerably lower levels (Fig. 5D). These findings demonstrate that 2BP can alleviate severe lipid deposition mediated
288 by CD36 in $Nrf1\alpha^{-/-}$ cells.

289 Further examination revealed that transcriptional expression levels of the inflammatory cytokines IL-6 and TNFα
290 in $Nrf1\alpha^{-/-}$ cells were significantly suppressed or even completely abolished by 2BP when compared to wild-type
291 controls (Fig. 5E). Also, the basal IL-6 abundance and active phosphorylated NFκB were repressed by 2BP (Fig. 5C). This
292 implies that the inflammatory response to the loss of $Nrf1\alpha^{-/-}$ may be prevented by 2BP. Flow cytometry analysis
293 showed a marked accumulation of the intracellular ROS (involved in the inflammatory response) in $Nrf1\alpha^{-/-}$ cells (Fig.
294 5F, *left panel,* with an enhanced peak shifted to the right), but such severe ROS accumulation was also obviously
295 mitigated by 2BP (Fig. 5F, *right panel,* with a reduced peak shifted to the left). However, no similar ROS changes were
296 observed in $Nrf1/2^{+/+}$ cells (Fig. 5F, *middle panel*). Statistical analysis of these data are shown graphically in Fig. 5G.
297 However, ROS accumulation in the mitochondria of $Nrf1\alpha^{-/-}$ cells (measured using a MitoTracker Red CMXRos ROS test
298 kit) was only partially reduced by 2BP (Fig. S2F). Collectively, these indicate that 2BP can enable effective alleviation of
299 the inflammatory accumulation of lipids by enhanced biosynthesis and uptake of fatty acids through up-regulation of
300 CD36 in $Nrf1\alpha^{-/-}$ cells. This occurs concomitantly with a reduction of ROS by 2BP to mitigate the inflammatory response
301 caused by loss of Nrf1α.

3.6 The expression of key genes governing lipid catabolism is transcriptionally regulated by Nrf1 through the ARE sites.

304 Clearly, the consensus *ARE* sequence (5'-TGAC/GnnnGC-3') is known as a *cis*-acting enhancer that drives
305 transcription of genes regulated by Nrf1 and Nrf2 in response to changes in the cellular redox status (i.e., increased
306 production of free radical species including ROS from disordered cell metabolism) or to pro-oxidant xenobiotics that
307 are thiol reactive and mimic oxidative insults [31]. Nrf2 was well documented as an interface between redox and
308 intermediary metabolism [32], so as to protect the liver against steatosis by inhibiting lipogenesis and promoting fatty
309 acid oxidation, but also to exerts its dual role in nonalcoholic fatty liver disease [33]. This may be explained by
310 activation of *ARE*-driven transcription factors that are responsible for regulating the adipocyte differentiation and
311 adipogenesis (e.g., CCAAT/enhancer-binding protein β, peroxisome proliferator-activated receptor-γ, aryl hydrocarbon
312 receptor, and retinoid X receptor-α) and by protection against redox-dependent inactivation of metabolic enzymes
313 (e.g., 3-hydroxy-3-methylglutaryl-CoA reductase). Besides, Nrf1 was also shown to mediate the expression of lipid
314 metabolism-related genes *Lipin1, PGC-1β* [34] and *CD36* [35] by directly binding to the consensus *ARE* sites in their
315 regulatory regions. Here, ChIP-sequencing date obtained from the Encode database (Fig. 6E) showed several peak
316 signals representing the activity of Nrf1 binding to multiple *ARE* sites located within the promoter regions of *ATGL,*
317 *PGC-1α, PPARα* and *PPARγ.* Such Nrf1-binding details of the ChIP-sequecing data were also provided (Fig. S3, *A to D*).
318 Further experimental results demonstrated that co-expression of Nrf1 may lead to a certain transactivation activity of
319 some *ARE*-driven luciferase reporter genes (Fig. 6, *B to E*). These ARE sequences were selected from within the 4k-bp
320 promoter regions of *ATGL, PGC-1α, PPARα* and *PPARγ,* each of which was subcloned into the pGL3-Promoter vector to
321 give rise to those indicated *ARE-Luc* reporter genes as indicated (in Fig. 6F and Table 2). However, Nrf1-mediated

322   transcriptional ability of *ARE-Luc* reporter genes was modestly augmented to less than two-fold changed degrees. This
323   implies that transcriptional expression of lipid catabolism-related genes may be finely tuned by Nrf1 within a certain
324   robust homeostatic extent.

325   **4. Discussion**

326   In the present study, we have provided new evidence unraveling the different or even opposite effects of Nrf1 and
327   Nrf2 on the human lipid metabolism, in addition to our previously reported effects on glucose metabolism[19, 36], the
328   protein homeostasis (proteostasis) [17, 37] and the redox balance and signaling control [38-40]. Thereby, it is of crucial
329   significance to note that the experimental cell model of $Nrf1\alpha^{-/-}$ with pathophysiological phenotypes appears to
330   largely resemble those manifested by the liver-specific $Nrf1$ knockout mice. Such loss of $Nrf1^{-/-}$ results in the
331   spontaneous development of NASH and ultimately liver cancer, which is attributed to the rapid accumulation of a large
332   volume of lipids, as a key etiology, in the pathological process [9]. Herein, our experimental evidence demonstrated
333   that lipids (i.e., triglyceride contents) were markedly deposited in distinct sizes of the intracellular lipid droplets and
334   widely distributed within the human $Nrf1\alpha^{-/-}$ hepatoma cells, particularly following treatment with oleic and palmitic
335   acids (Fig. 1, and also see Fig. S4). By contrast, there was a reduced abundance of lipid droplets in $Nrf2^{-/-}$ cells, even
336   after they were treated with oleic acids.
337   Interestingly, we have also discovered that abnormal lipid deposition in $Nrf1\alpha^{-/-}$ cells was substantially blocked by
338   a palmitic acid analogue, i.e., 2-bromopalmitate (2BP, Fig. 5), through significant down-regulation of CD36 (acting as an
339   essential translocator of fatty acids). The concomitant inflammatory response and oxidative stress were ameliorated
340   significantly by 2-bromopalmitate. As a preventive consequence, those key inflammatory cytokines and the
341   transcription factor NFκB were markedly down-regulated, following reduction of ROS and lipids, in 2BP-treated
342   $Nrf1\alpha^{-/-}$ cells. However, it should also be noted that in addition to the secondary production of ROS stimulated by the
343   accumulation of lipids, the primary production of ROS was partially caused by $Nrf1\alpha^{-/-}$ cell-autonomous
344   reprogramming of the redox metabolism [19, 36, 39]. Thereby, such portion of $Nrf1\alpha^{-/-}$ cell-autonomous yield of ROS
345   (particularly in the mitochondria) is inferable to be largely unaffected by 2BP (Figs. 5F & S2F). The evidence presented
346   herein also shows that, even though the putative concomitant ROS resulting from severe lipid deposition may be
347   diminished by 2BP (as an irreversible inhibitor of many membrane-associated enzymes), the oxidative stress is not
348   completely mitigated and recovered to the levels measured from wild-type cells. This palmitic acid analogue 2BP was
349   originally identified as an inhibitor of β-oxidation, but further studies reported that it can also inhibit fatty acyl CoA
350   ligase, glycerol-3-phosphate acyltransferase, mono-, di- and tri-acylglycerol transferases [41]. Therefore, 2BP is thought
351   to block protein palmitoylation by inhibiting such a family of those conserved protein acyl transferases (PATs). Notably,
352   2BP prevents the incorporation of palmitate into the putative palmitoylated proteins, which may actually reflect
353   alkylation by 2BP at the palmitoylation site, but also seems to reduce palmitoylation of indicated proteins. When used
354   to describe an alkynyl analogue, 2BP also serves a non-selective probe with other targets beyond the palmitoyl
355   transferases [42]. Given the ubiquitous usage of 2BP in a large number of studies published, it should have a significant
356   ramification on the palmitoylation area [43]. For instance, CD36 palmitoylation causes an increase in its trafficking and
357   also cell-surface location of adipocytes, which makes oleate uptake easier [44]. Once palmitoylation of CD36 is
358   inhibited, its hydrophobicity and accessibility to the plasma membrane are accordingly decreased, which results in less
359   binding and absorption of long-chain fat acids [45]. This implies that palmitoylated CD36, as a cognate key target of
360   Nrf1, plays a crucial role in fat acid and other lipid metabolism. Consistently, 2-BP was *de facto* employed to effectively

361   prevent CD36 palmitoylation modification [46].

362   Here, we have also provided evidence revealing that abnormal accumulation of lipids in $Nrf1\alpha^{-/-}$ cells resulted

363   from incremented uptake of fatty acids through constitutive activation of the PI3K-AKT-mTOR signaling pathway

364   leading to up-regulation of CD36. The CD36-augmented uptake of lipids is fully consistent with the results obtained

365   from the tissue-specific $Nrf1^{-/-}$ mice [10, 35]. These two independent groups further showed that Nrf1 is essential for

366   controlling the translocation of fatty acids and the cystine/cysteine contents by governing a complex hierarchical

367   regulatory network in redox and lipid metabolism. In addition to CD36, there are also some members of the

368   cytochrome family, such as Cyp 4A, were also up-regulated by the loss of $Nrf1^{-/-}$, thus leading to the generation of ROS

369   from the oxidative metabolism of fatty acids, in the murine deficient liver cells [10, 11]. Besides, we also previously

370   showed that Nrf1 and Nrf2 contribute to dual opposing regulation of the PTEN-AKT signaling to be selectively

371   repressed or activated in the pathogenesis of NASH and liver cancer [17]. In the present study, we further validated

372   that the extended PI3K-AKT-mTOR signaling to the inflammatory marker COX2, as well as the key inflammatory

373   responsive factors along with CD36, was also constitutively activated by such loss of Nrf1α in human hepatoma cells.

374   In this study, we have provided more insight into the molecular mechanisms of how $Nrf1\alpha^{-/-}$ deficiency is involved

375   in lipid metabolism disorders, along with the relevant pathway of enzymatic reactions leading to lipid deposition

376   during development of NASH and hepatoma. Our evidence demonstrates that the key enzymes FASN, SCD1 and ACCα

377   and the transcription factor SREBP1 (involved in the *de novo* biosynthesis of lipids) were significantly up-regulated in

378    $Nrf1\alpha^{-/-}$ cells (with hyper-active Nrf2 retained). However, they were unaffected or even down-regulated by inactivation

379   of Nrf2 in $Nrf2^{-/-}$ cells. Further experimental evidence showed that such up-regulation of the lipid biosynthesis

380   pathway by $Nrf1\alpha^{-/-}$ deficiency may occur through the JNK-Nrf2-AP1 signaling. An explanation for the results regarding

381   Nrf2 may be attributed to the heterodimeric formation of Nrf2 with each of sMaf or other bZIP proteins, thereby

382   competing with JUN and FOS against another cognate heterodimeric AP1 factor for selective physical binding to the

383   potential *ARE* consensus sites within their target gene promoter regions [47].

384   We also found that ATGL and the nuclear receptor PPAR-PGC1 signaling towards the lipid oxidative decomposition

385   pathway were markedly down-regulated in $Nrf1\alpha^{-/-}$ cells, but they were unaffected or even up-regulated in $Nrf2^{-/-}$ cells.

386   The activation of the PPAR-PGC1 signaling was also supported by the evidence obtained from the tissue-specific $Nrf1^{-/-}$

387   mice [12, 48]. Hirotsu *et al* [12] showed that liver-specific *Nrf1* deficiency cannot only lead to decreased expression of

388   Lipin1 and PGC-1β, but conversely, the presence of Nrf1 enabled the CNC-bZIP factor to directly mediate

389   transcriptional activation of *Lipin1* and *PGC-1β* by binding to the ARE sequences in their promoter regions. Collectively,

390   this indicates that Nrf1 is predominantly essential for regulating the critical genes involved in lipid catabolism. Upon

391   loss of $Nrf1\alpha^{-/-}$, constitutive activation of the PPAR-PGC1 signaling cascades is implicated in the severe aberrant

392   accumulation of lipids. The resulting metabolic pathological process may be significantly prevented by 2BP, because

393   this palmitic acid analogue has also been shown to serve as a ligand of PPARδ receptor involved in the fatty acid

394   oxidation [30], although the detailed molecular mechanisms remain unclear.

395   In summary, this work demonstrates that both Nrf1 and Nrf2 make different or even opposite contributions to the

396   intracellular lipid metabolism, as illustrated in a model (Fig. 6G). Upon knockout of Nrf1α, the *de novo* biosynthesis of

397   lipids is incremented by significant induction of the JNK-Nrf2-AP1 signaling pathway in $Nrf1\alpha^{-/-}$ cells, whereas the lipid

398   oxidative decomposition pathway was down-regulated by the PPAR-PGC1 signaling cascades. $Nrf1\alpha^{-/-}$ cell-autonomous

399   activation of the PI3K-AKT-mTOR signaling towards up-regulation of CD36 leads to augmented uptake of fatty acids.

400 Taken altogether, these results lead to severe accumulation of lipids deposited as lipid droplets. By contrast, $Nrf2^{-/-}$
401 cells gave rise to rather decreases in both lipid synthesis and uptake capacity, along with enhanced oxidative
402 metabolism of fatty acids. Importantly, such $Nrf1\alpha^{-/-}$-leading lipid metabolism disorders and the relevant inflammatory
403 responses are substantially rescued by 2BP, probably through blocking palmitoylation of CD36 (as a target of Nrf1).
404 Overall, this study provides a novel potential strategy for chemoprevention of the inflammatory transformation into
405 malignant cancer and the relevant treatment by precision targeting of Nrf1, Nrf2 alone or both in translational
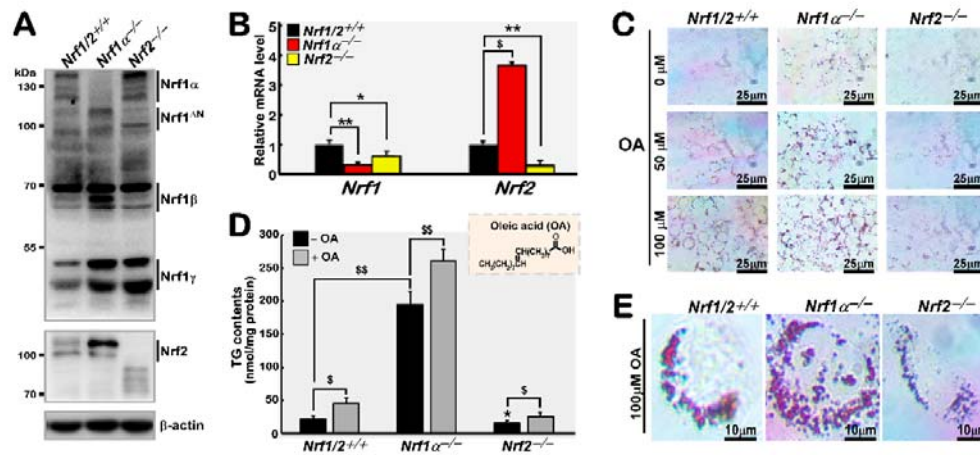406 medicine.

References

1. Cao, H., Gerhold, K., Mayers, J. R., Wiest, M. M., Watkins, S. M. & Hotamisligil, G. S. (2008) Identification of a lipokine, a lipid hormone linking adipose tissue to systemic metabolism, *Cell*. **134**, 933-44.
2. Parker, B. L., Calkin, A. C., Seldin, M. M., Keating, M. F., Tarling, E. J., Yang, P., Moody, S. C., Liu, Y., Zerenturk, E. J., Needham, E. J., Miller, M. L., Clifford, B. L., Morand, P., Watt, M. J., Meex, R. C. R., Peng, K. Y., Lee, R., Jayawardana, K., Pan, C., Mellett, N. A., Weir, J. M., Lazarus, R., Lusis, A. J., Meikle, P. J., James, D. E., de Aguiar Vallim, T. Q. & Drew, B. G. (2019) An integrative systems genetic analysis of mammalian lipid metabolism, *Nature*. **567**, 187-193.
3. Horton, J. D. (2008) Physiology. Unfolding lipid metabolism, *Science*. **320**, 1433-4.
4. Cheng, C., Zhuo, S. M., Zhang, B., Zhao, X., Liu, Y., Liao, C. L., Quan, J., Li, Z. Z., Bode, A. M., Cao, Y. & Luo, X. J. (2019) Treatment implications of natural compounds targeting lipid metabolism in nonalcoholic fatty liver disease, obesity and cancer, *Int J Biol Sci*. **15**, 1654-1663.
5. Alannan, M., Fayyad-Kazan, H., Trezeguet, V. & Merched, A. (2020) Targeting Lipid Metabolism in Liver Cancer, *Biochemistry-Us*. **59**, 3951-3964.
6. Santos, C. R. & Schulze, A. (2012) Lipid metabolism in cancer, *Febs J*. **279**, 2610-23.
7. Walther, T. C. & Farese, R. V., Jr. (2012) Lipid droplets and cellular lipid metabolism, *Annu Rev Biochem*. **81**, 687-714.
8. Zhang, Y. & Xiang, Y. (2016) Molecular and cellular basis for the unique functioning of Nrf1, an indispensable transcription factor for maintaining cell homoeostasis and organ integrity, *Biochem J*. **473**, 961-1000.
9. Parola, M. & Novo, E. (2005) Nrf1 gene expression in the liver: A single gene linking oxidative stress to NAFLD, NASH and hepatic tumours, *J Hepatol*. **43**, 1096-1097.
10. Tsujita, T., Peirce, V., Baird, L., Matsuyama, Y., Takaku, M., Walsh, S. V., Griffin, J. L., Uruno, A., Yamamoto, M. & Hayes, J. D. (2014) Transcription Factor Nrf1 Negatively Regulates the Cystine/Glutamate Transporter and Lipid-Metabolizing Enzymes, *Mol Cell Biol*. **34**, 3800-3816.
11. Xu, Z. R., Chen, L. Y., Leung, L., Yen, T. S. B., Lee, C. & Chan, J. Y. (2005) Liver-specific inactivation of the Nrf1 gene in adult mouse leads to nonalcoholic steatohepatitis and hepatic neoplasia, *P Natl Acad Sci USA*. **102**, 4120-4125.
12. Hirotsu, Y., Hataya, N., Katsuoka, F. & Yamamoto, M. (2012) NF-E2-Related Factor 1 (Nrf1) Serves as a Novel Regulator of Hepatic Lipid Metabolism through Regulation of the Lipin1 and PGC-1 beta Genes, *Mol Cell Biol*. **32**, 2760-2770.
13. Sharma, R. S., Harrison, D. J., Kisielewski, D., Cassidy, D. M., McNeilly, A. D., Gallagher, J. R., Walsh, S. V., Honda, T., McCrimmon, R. J., Dinkova-Kostova, A. T., Ashford, M. L. J., Dillon, J. F. & Hayes, J. D. (2018) Experimental Nonalcoholic Steatohepatitis and Liver Fibrosis Are Ameliorated by Pharmacologic Activation of Nrf2 (NF-E2 p45-Related Factor 2), *Cell Mol Gastroenterol Hepatol*. **5**, 367-398.

451   14.   Kamisako, T., Tanaka, Y., Kishino, Y., Ikeda, T., Yamamoto, K., Masuda, S. & Ogawa, H. (2014) Role of Nrf2 in
452   the alteration of cholesterol and bile acid metabolism-related gene expression by dietary cholesterol in high fat-fed
453   mice, *J Clin Biochem Nutr.* **54**, 90-4.
454   15.   Huang, J. S., Tabbi-Anneni, I., Gunda, V. & Wang, L. (2010) Transcription factor Nrf2 regulates SHP and
455   lipogenic gene expression in hepatic lipid metabolism, *Am J Physiol-Gastr L.* **299**, G1211-G1221.
456   16.   Zhang, L., Dasuri, K., Fernandez-Kim, S. O., Bruce-Keller, A. J. & Keller, J. N. (2016) Adipose-specific ablation
457   of Nrf2 transiently delayed high-fat diet-induced obesity by altering glucose, lipid and energy metabolism of male mice,
458   *Am J Transl Res.* **8**, 5309-+.
459   17.   Qiu, L., Wang, M., Hu, S. F., Ru, X. F., Ren, Y. G., Zhang, Z. W., Yu, S. W. & Zhang, Y. G. (2018) Oncogenic
460   Activation of Nrf2, Though as a Master Antioxidant Transcription Factor, Liberated by Specific Knockout of the
461   Full-Length Nrf1 alpha that Acts as a Dominant Tumor Repressor, *Cancers.* **10**.
462   18.   Zhang, Y. G., Lucocq, J. M. & Hayes, J. D. (2009) The Nrf1 CNC/bZIP protein is a nuclear envelope-bound
463   transcription factor that is activated by t-butyl hydroquinone but not by endoplasmic reticulum stressors, *Biochemical
464   Journal.* **418**, 293-310.
465   19.   Zhu, Y. P., Zheng, Z., Hu, S., Ru, X., Fan, Z., Qiu, L. & Zhang, Y. (2019) Unification of Opposites between Two
466   Antioxidant Transcription Factors Nrf1 and Nrf2 in Mediating Distinct Cellular Responses to the Endoplasmic Reticulum
467   Stressor Tunicamycin, *Antioxidants.* **9**.
468   20.   Bathish, B., Robertson, H., Dillon, J. F., Dinkova-Kostova, A. T. & Hayes, J. D. (2022) Nonalcoholic
469   steatohepatitis and mechanisms by which it is ameliorated by activation of the CNC-bZIP transcription factor Nrf2, *Free
470   Radic Biol Med.* **188**, 221-261.
471   21.   Snaebjornsson, M. T., Janaki-Raman, S. & Schulze, A. (2020) Greasing the Wheels of the Cancer Machine:
472   The Role of Lipid Metabolism in Cancer, *Cell Metab.* **31**, 62-76.
473   22.   Kronenberg, F., Schoenborn, V., Heid, I. M., Vollmert, C., Lingenhel, A., Adams, T. D., Hopkins, P. N., Illig, T.,
474   Zimmermann, R., Zechner, R. & Hunt, S. C. (2005) The ATGL gene is associated with free fatty acids, trigylcerides and
475   type 2 diabetes, *Genet Epidemiol.* **29**, 259-259.
476   23.   Memon, R. A., Tecott, L. H., Nonogaki, K., Beigneux, A., Moser, A. H., Grunfeld, C. & Feingold, K. R. (2000)
477   Up-regulation of peroxisome proliferator-activated receptors (PPAR-alpha) and PPAR-gamma messenger ribonucleic
478   acid expression in the liver in murine obesity: Troglitazone induces expression of PPAR-gamma-responsive adipose
479   tissue-specific genes in the liver of obese diabetic mice, *Endocrinology.* **141**, 4021-4031.
480   24.   Miura, S., Kai, Y., Kamei, Y. & Ezaki, O. (2008) Isoform-specific increases in murine skeletal muscle
481   peroxisome proliferator-activated receptor-gamma coactivator-1 alpha (PGC-1 alpha) mRNA in response to beta
482   2-adrenergic receptor activation and exercise, *Endocrinology.* **149**, 4527-4533.
483   25.   Li, J., Shen, H., Owens, G. K. & Guo, L. W. (2022) SREBP1 regulates Lgals3 activation in response to
484   cholesterol loading, *Mol Ther Nucleic Acids.* **28**, 892-909.
485   26.   Li, Z., Feng, S., Zhou, L., Liu, S. & Cheng, J. (2016) NS5ATP6 modulates intracellular triglyceride content
486   through FGF21 and independently of SIRT1 and SREBP1, *Biochem Biophys Res Commun.* **475**, 133-9.
487   27.   Gao, N., Zhang, Z., Jiang, B. H. & Shi, X. L. (2003) Role of PI3K/AKT/mTOR signaling in the cell cycle
488   progression of human prostate cancer, *Biochem Bioph Res Co.* **310**, 1124-1132.
489   28.   Wang, C., Hu, L., Zhao, L., Yang, P., Moorhead, J. F., Varghese, Z., Chen, Y. & Ruan, X. Z. (2014) Inflammatory
490   stress increases hepatic CD36 translational efficiency via activation of the mTOR signalling pathway, *Plos One.* **9**,
491   e103071.
492   29.   Cao, D. Y., Luo, J., Chen, D. K., Xu, H. F., Shi, H. P., Jing, X. Q. & Zang, W. J. (2016) CD36 regulates
493   lipopolysaccharide-induced signaling pathways and mediates the internalization of Escherichia coli in cooperation with
494   TLR4 in goat mammary gland epithelial cells, *Sci Rep-Uk.* **6**.
495   30.   Berger, J. & Moller, D. E. (2002) The mechanisms of action of PPARs, *Annu Rev Med.* **53**, 409-435.
496   31.   Zhang, Y. (2009) Molecular and cellular control of the Nrf1 transcription factor: An integral membrane
497   glycoprotein, *Vdm Verlag Dr Müller Publishing House.* **Germany (May 2009). The first edition**   pp1-264.
498   32.   Hayes, J. D. & Dinkova-Kostova, A. T. (2014) The Nrf2 regulatory network provides an interface between
499   redox and intermediary metabolism, *Trends Biochem Sci.* **39**, 199-218.
500   33.   Chambel, S. S., Santos-Goncalves, A. & Duarte, T. L. (2015) The Dual Role of Nrf2 in Nonalcoholic Fatty Liver
501   Disease: Regulation of Antioxidant Defenses and Hepatic Lipid Metabolism, *Biomed Res Int.* **2015**, 597134.
502   34.   Finck, B. N., Gropler, M. C., Chen, Z., Leone, T. C., Croce, M. A., Harris, T. E., Lawrence, J. C., Jr. & Kelly, D. P.
503   (2006) Lipin 1 is an inducible amplifier of the hepatic PGC-1alpha/PPARalpha regulatory pathway, *Cell Metab.* **4**,
504   199-210.
505   35.   Widenmaier, S. B., Snyder, N. A., Nguyen, T. B., Arduini, A., Lee, G. Y., Arruda, A. P., Saksi, J., Bartelt, A. &
506   Hotamisligil, G. S. (2017) NRF1 Is an ER Membrane Sensor that Is Central to Cholesterol Homeostasis, *Cell.* **171**,
507   1094-1109 e15.
508   36.   Zhu, Y. P., Zheng, Z., Xiang, Y. & Zhang, Y. (2020) Glucose Starvation-Induced Rapid Death of
509   Nrf1alpha-Deficient, but Not Nrf2-Deficient, Hepatoma Cells Results from Its Fatal Defects in the Redox Metabolism
510   Reprogramming, *Oxid Med Cell Longev.* **2020**, 4959821.
511   37.   Chen, J., Wang, M., Xiang, Y., Ru, X., Ren, Y., Liu, X., Qiu, L. & Zhang, Y. (2020) Nrf1 Is Endowed with a
512   Dominant Tumor-Repressing Effect onto the Wnt/beta-Catenin-Dependent and Wnt/beta-Catenin-Independent
513   Signaling Networks in the Human Liver Cancer, *Oxid Med Cell Longev.* **2020**, 5138539.
514   38.   Zhang, S., Deng, Y., Xiang, Y., Hu, S., Qiu, L. & Zhang, Y. (2020) Synergism and Antagonism of Two Distinct, but

515 Confused, Nrf1 Factors in Integral Regulation of the Nuclear-to-Mitochondrial Respiratory and Antioxidant
516 Transcription Networks, *Oxid Med Cell Longev.* **2020**, 5097109.
517   39.   Wufur, R., Fan, Z., Liu, K. & Zhang, Y. (2021) Differential yet integral contributions of Nrf1 and Nrf2 in the
518 human antioxidant cytoprotective response against tert-butylhydroquinone as a pro-oxidative stressor, *bioRxiv.*
519 **2021.06.05.447190**, doi: https://doi.org/10.1101/2021.06.05.447190.
520   40.   Hu, S., Feng, J., Wang, M., Wufuer, R., Liu, K., Zhang, Z. & Zhang, Y. (2022) Nrf1 is an indispensable
521 redox-determining factor for mitochondrial homeostasis by integrating multi-hierarchical regulatory networks, *Redox*
522 *Biol.* **57**, 102470.
523   41.   RA, C., P, R., RJ, F. & ES, B. (1992) 2-Bromopalmitoyl-CoA and 2-bromopalmitate: promiscuous inhibitors of
524 membrane-bound enzymes, *Biochim Biophys Acta.* **1125 %J Biochimica et biophysica acta**.
525   42.   JF, C. & PK, T. (1972) Specific inhibition of mitochondrial fatty acid oxidation by 2-bromopalmitate and its
526 coenzyme A and carnitine esters, *Biochem J.* **129 %J The Biochemical journal**.
527   43.   Davda, D., El Azzouny, M. A., Tom, C. T., Hernandez, J. L., Majmudar, J. D., Kennedy, R. T. & Martin, B. R.
528 (2013) Profiling targets of the irreversible palmitoylation inhibitor 2-bromopalmitate, *ACS Chem Biol.* **8**, 1912-7.
529   44.   Wang, J., Hao, J. W., Wang, X., Guo, H., Sun, H. H., Lai, X. Y., Liu, L. Y., Zhu, M., Wang, H. Y., Li, Y. F., Yu, L. Y.,
530 Xie, C., Wang, H. R., Mo, W., Zhou, H. M., Chen, S., Liang, G. & Zhao, T. J. (2019) DHHC4 and DHHC5 Facilitate Fatty Acid
531 Uptake by Palmitoylating and Targeting CD36 to the Plasma Membrane, *Cell Rep.* **26**, 209-221 e5.
532   45.   Zhao, L., Zhang, C., Luo, X., Wang, P., Zhou, W., Zhong, S., Xie, Y., Jiang, Y., Yang, P., Tang, R., Pan, Q., Hall, A.
533 R., Luong, T. V., Fan, J., Varghese, Z., Moorhead, J. F., Pinzani, M., Chen, Y. & Ruan, X. Z. (2018) CD36 palmitoylation
534 disrupts free fatty acid metabolism and promotes tissue inflammation in non-alcoholic steatohepatitis, *J Hepatol.* **69**,
535 705-717.
536   46.   Zhang, Y., Dong, D., Xu, X., He, H., Zhu, Y., Lei, T. & Ou, H. (2022) Oxidized high-density lipoprotein promotes
537 CD36 palmitoylation and increases lipid uptake in macrophages, *J Biol Chem.* **298**, 102000.
538   47.   Newman, J. R. & Keating, A. E. (2003) Comprehensive identification of human bZIP interactions with
539 coiled-coil arrays, *Science.* **300**, 2097-101.
540   48.   Hou, Y., Liu, Z., Zuo, Z., Gao, T., Fu, J., Wang, H., Xu, Y., Liu, D., Yamamoto, M., Zhu, B., Zhang, Y., Andersen, M.
541 E., Zhang, Q. & Pi, J. (2018) Adipocyte-specific deficiency of Nfe2l1 disrupts plasticity of white adipose tissues and
542 metabolic homeostasis in mice, *Biochem Biophys Res Commun*.
543   49.   Zheng, Z., Wang, M., Hu, S., Deng, R., Feng, J. & Zhang, Y. (2021) The inflammatory accumulation of lipids
544 and ROS in human Nrf1α-deficient hepatoma cells is ameliorated by 2-bromopalmitate, *BioRxiv*, 2021.09.29.462358;
545 doi: https://doi.org/10.1101/2021.09.29.462358
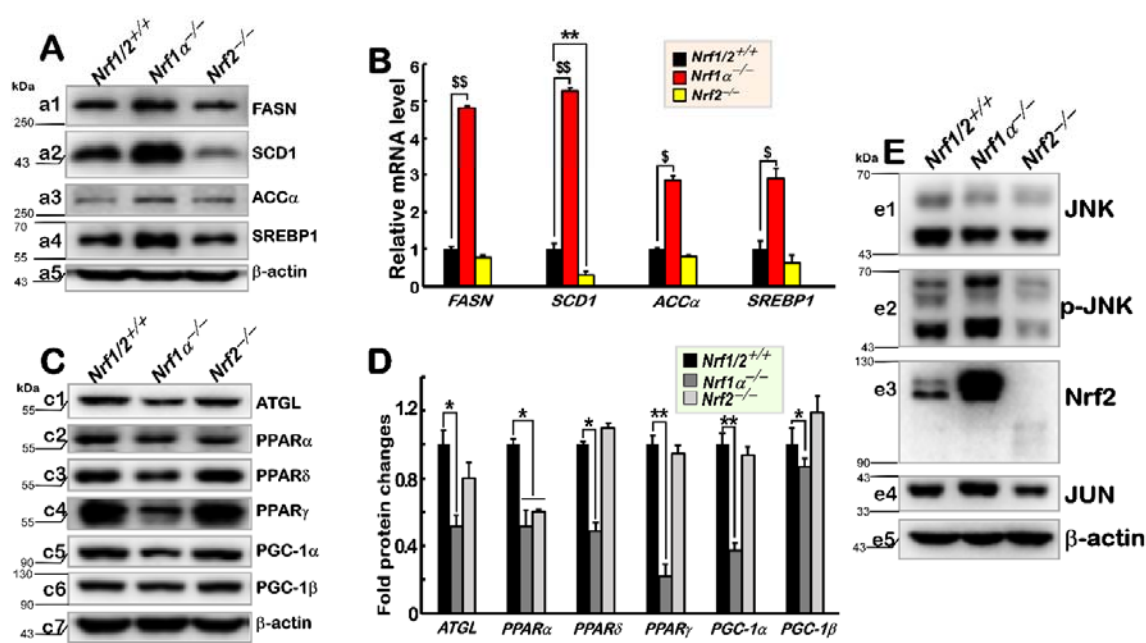
546

547 **Figure legends**

Figure 1

Figure 1. Significant differences between Nrf1 and Nrf2 in lipid metabolism are observed in their genotypic knockout cell lines. (A) Nrf1 and Nrf2 protein levels in three different genotypic cell lines $Nrf1/2^{+/+}$, $Nrf1\alpha^{-/-}$ and $Nrf2^{-/-}$ were determined by Western blotting using specific antibodies. β-actin was used as a loading control. (B) mRNA expression levels of both Nrf1 and Nrf2 were examined by real-time qPCR analysis of $Nrf1/2^{+/+}$, $Nrf1\alpha^{-/-}$ and $Nrf2^{-/-}$ cell lines. The results were then calculated as fold changes (mean ± S.D) with significant increases ($, $P < 0.01$) and significant de-creases (*, $P < 0.05$; **, $P < 0.01$). (C) The triglyceride (TG) contents were measured after $Nrf1/2^{+/+}$, $Nrf1\alpha^{-/-}$ and $Nrf2^{-/-}$ cell lines were pretreated with 100 μmol/L oleic acid (OA). The results were then calculated as a concentration of nmol *per* mg of protein, with significant

16

555   increases ($, *P* < 0.01; $$, *P* < 0.001) or significant decreases (*, *P* < 0.05). (D) The same cell lines were further subjected to

556   pretreatment with distinct concentrations of oleic acid (OA), followed by the oil red O staining, and photographed using a

557   microscope (scale bar = 25 μm), with higher resolution imaging of the same cells that had been treated as described above (E,

558   scale bar = 10 μm). The statistical significances were determined by using the Student's *t*-test or MANOVA.

Figure 2

559

560 **Figure 2. Different expression levels of lipid metabolism-related genes mediated by Nrf1 and Nrf2 in distinct genotypic cell**

561 **lines.** (A) Different protein levels of key genes involved in the *de novo* biosynthesis of lipids in *Nrf1/2*$^{+/+}$, *Nrf1α*$^{-/-}$ and *Nrf2*$^{-/-}$

562 cell lines were determined by Western blotting. β-actin was used as a loading control. (B) Different mRNA expression levels

563 of the indicated genes were determined by real-time qPCR. The results were calculated as fold changes (mean ± S.D) with

564 significant increases ($, *P* < 0.01; $$, *P* < 0.001) or significant decreases (**, *P* < 0.01). (C) The protein expression abundances

565 of those key enzymes and transcription factors involved in the lipid catabolism were evaluated by Western blotting. (D) The

566 intensity of all indicated immunoblots was calculated at fold changes (mean ± S.D) and shown graphically with significant

567 decreases (*, *P* < 0.05; **, *P* < 0.01). (E) Basal protein expression levels of JNK, p-JNK, Nrf2 and JUN were also examined in

568 *Nrf1/2*$^{+/+}$, *Nrf1α*$^{-/-}$ and *Nrf2*$^{-/-}$ cell lines. The statistical significances were determined by using *MANOVA*.

Figure 3

569
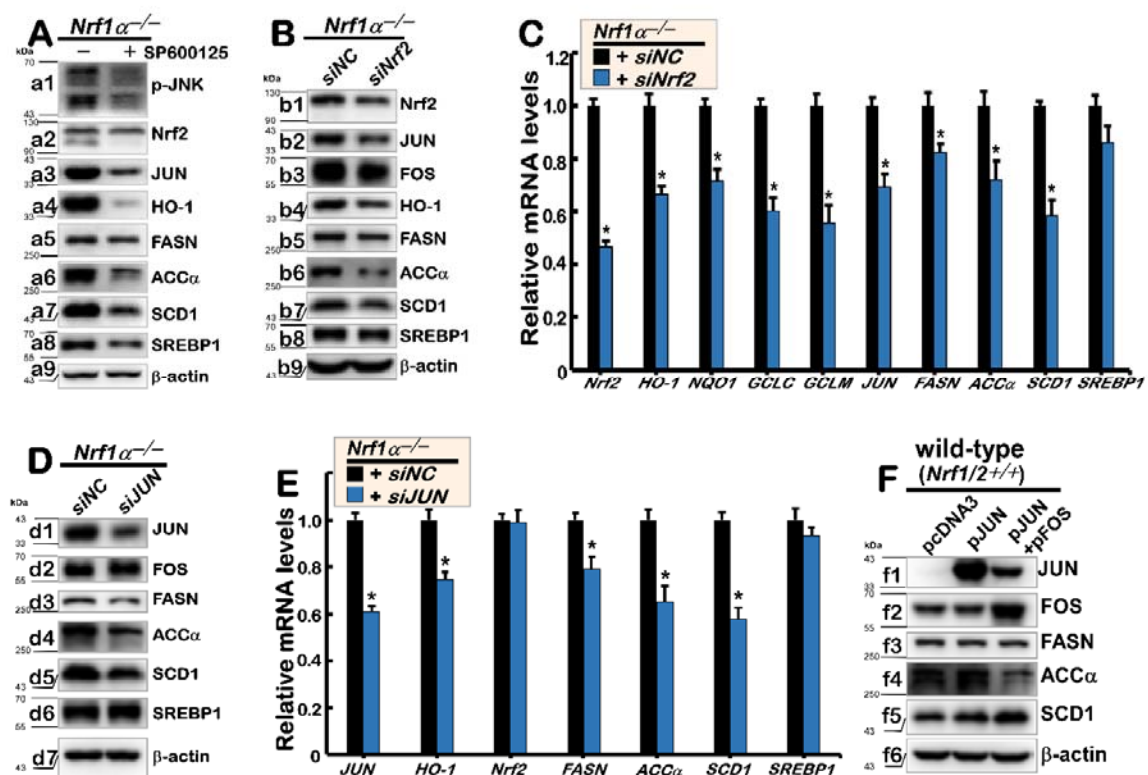
570 **Figure 3. The JNK-Nrf2-AP1 signaling pathway is required for increased expression of lipid synthesis genes in *Nrf1α*$^{-/-}$ cells.**

571 (A) *Nrf1α*$^{-/-}$ cells were treated with or without the JNK-specific inhibitor SP600125 (20 μmol/L) for 24 h and then subjected

572 to Western blot analysis of the JNK-Nrf2-AP1 lipid biosynthesis pathway proteins. (B, C) *Nrf1α*$^{-/-}$ cells were transfected with

573 *siNC* (small-interfering RNA negative control) or *siNrf2* (to specifically interfere with Nrf2), before being determined by (B)

574 Western blot analysis of the protein levels as described above or (C) real-time qPCR analysis of their mRNA expression levels.

575 The results were calculated as fold changes (mean ± S.D) with significant decreases (*, *P* < 0.05); statistical significances were

576 determined by using *MANOVA*. (D, E) *Nrf1α*$^{-/-}$ cells were transfected with *siJUN* (to specifically interfere with JUN) or *siNC*

577 and subjected to Western blotting analysis (D) and real-time qPCR analysis (E), as described above. (F) Wild-type *Nrf1/2*$^{+/+}$

578 cells transiently transfected with expression constructs for JUN (2 μg of DNA) alone or plus FOS (JUN+FOS, each 1 μg of DNA)

18

579 and then subjected to Western blotting analysis. β-actin was used as a loading control.

Figure 4
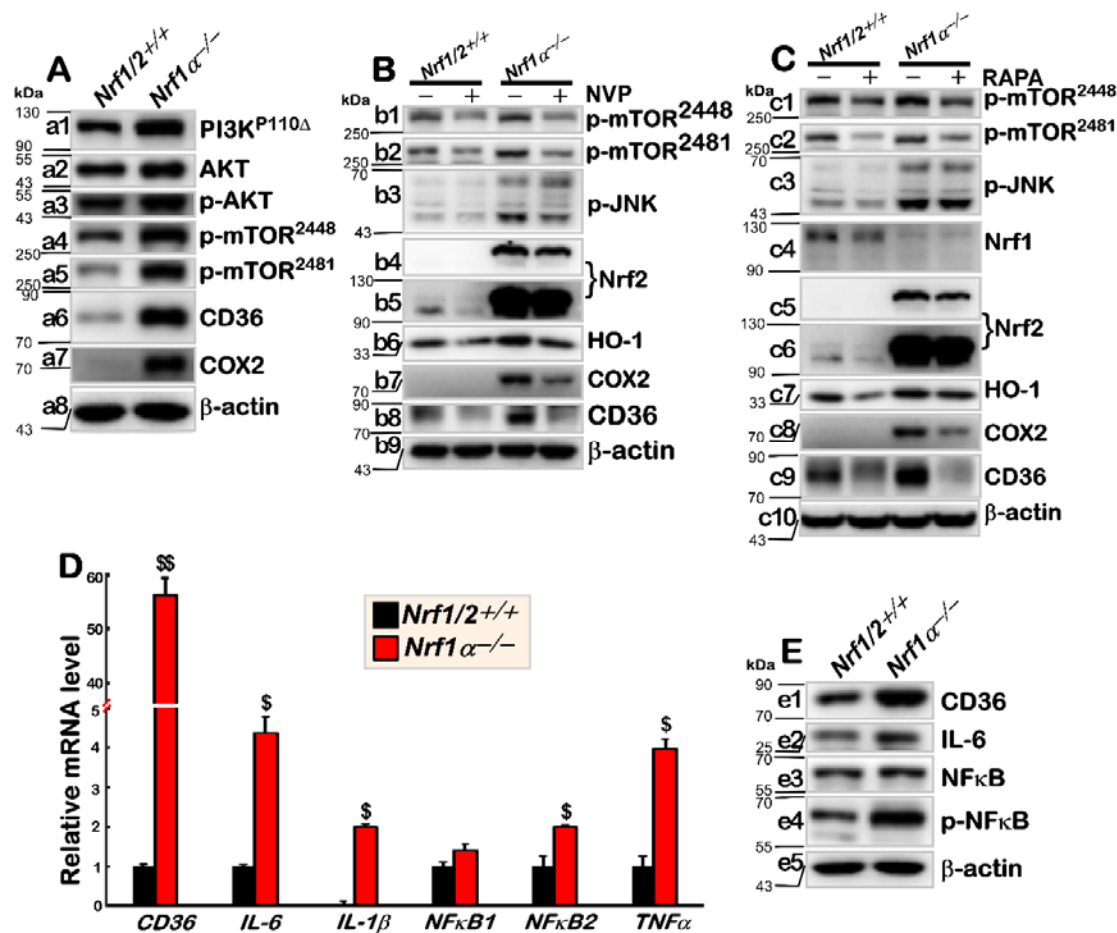
580

581 Figure 4. Nrf1α⁻/⁻ cell-autonomous up-regulation of CD36 and COX2 through the PI3K-AKT-mTOR sig-naling pathway.

582　(A) Western blotting analysis of indicated protein levels in *Nrf1/2*$^{+/+}$ and *Nrf1α*$^{-/-}$ cell lines as described in the legend for

583　Figure 3(B and C). (B) *Nrf1/2*$^{+/+}$ and *Nrf1α*$^{-/-}$ cells were treated with 0.5 μmol/L of the PI3K-specific inhibitor NVP-BKM120 or

584　(C) 200 nmol/L of the mTOR inhibitor rapamycin (RAPA) for 24 h before indicated protein levels were determined by Western

585　blotting analysis. (D) The mRNA expression levels of those key inflammatory factors and cytokines in *Nrf1/2*$^{+/+}$ and *Nrf1α*$^{-/-}$

586　cell lines were measured by real-time qPCR analysis. The results were calculated as fold changes (mean ± S.D) with significant

587　increases ($, $P < 0.01$; $$, $P < 0.001$). The statistical significances were determined by using the Student's *t*-test or MANOVA.

588　(E) Western blotting analysis of inflammatory factors and cytokines revealed changes in their protein expression levels in

589　*Nrf1/2*$^{+/+}$ and *Nrf1α*$^{-/-}$ cell lines. β-actin was used as a loading control.

Figure 5

590

Figure 5. Accumulation of lipids and ROS along with the inflammatory response in *Nrf1α*$^{-/-}$ cells are substantially

alleviated by 2BP. (A) The schematic shows the molecular structures of palmitic acid (PA) and 2-bromopalmitate (2BP). (B)

The triglyceride contents were measured following treatment of *Nrf1/2*$^{+/+}$ and *Nrf1α*$^{-/-}$ cell lines with 50 μmol/L 2BP. (C)

2BP-treated cell lines were subjected to Western blotting analysis of CD36, IL-6 and p-NFκB. (D) Oil red O staining of *Nrf1/2*$^{+/+}$

and *Nrf1α*$^{-/-}$ cell lines that had been treated with or without 2BP (scale bar = 10 μm). (E) Real-time qPCR analysis of *IL-6*,

NFκB1, *NFκB2* and *TNFα* mRNA expression levels. The data were calculated as fold changes (mean ± S.D) with a significant

increase ($, $P < 0.01$, relative to the wild-type controls), and another significant decrease (*, $P < 0.05$, when compared to

598   those measured from the untreated cells). (F) Flow cytometry determination of ROS in $Nrf1/2^{+/+}$ and $Nrf1\alpha^{-/-}$ cell lines that

599   had been treated with 2BP or without this this palmitic acid analogue, as described in the section of "Materials and

600   Methods". the results were also graphically shown in (E), along with statistical significances determined by using MANOVA (*,
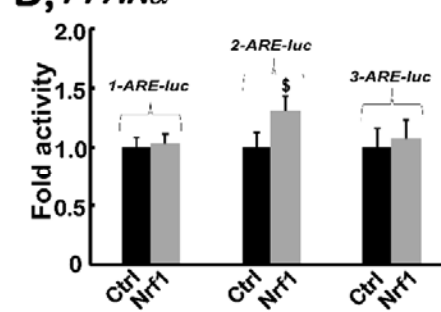
601    $P < 0.05$; $$, $P < 0.001$; ns, no significance).
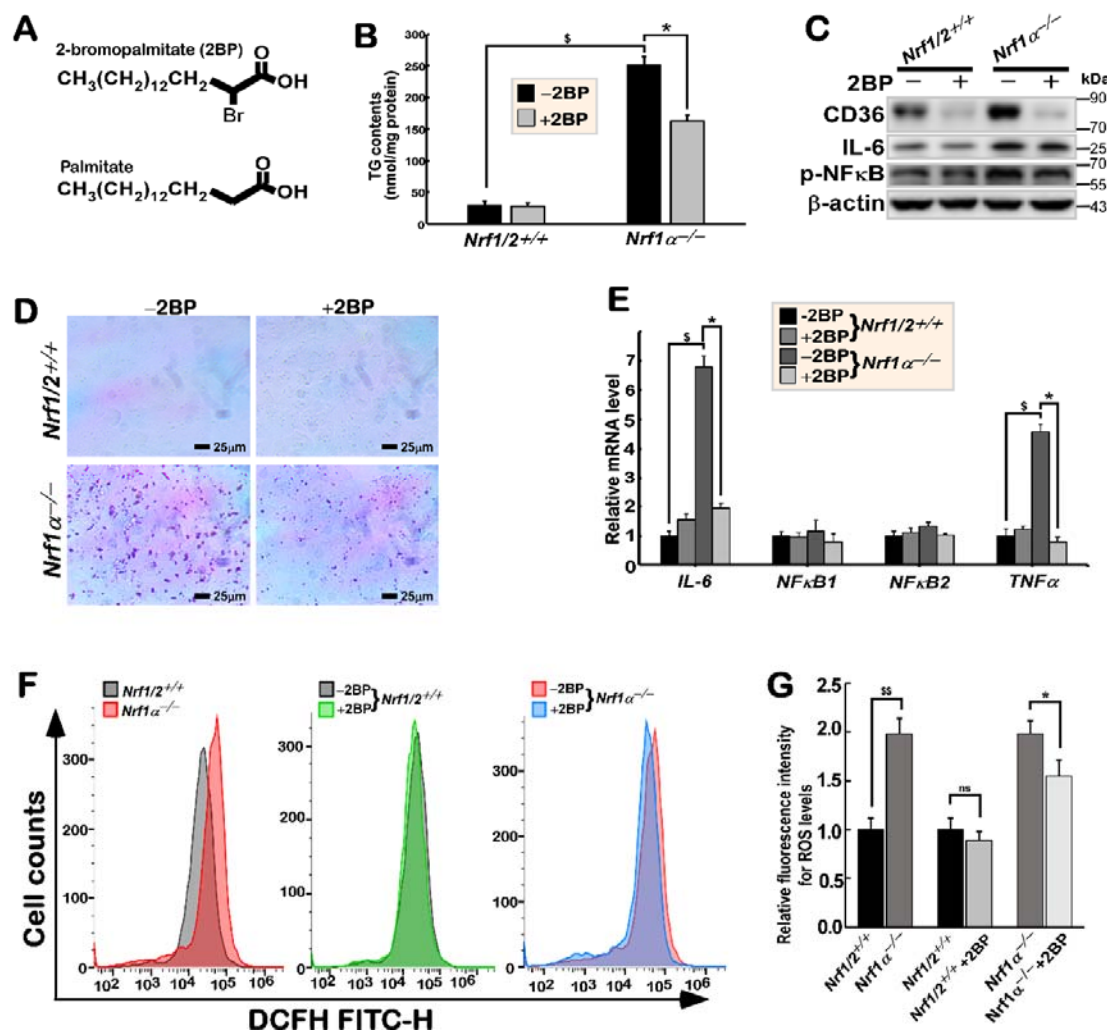
Figure 6

A, Nrf1-binding activity by ChIP-sequencing

B, ATGL

C, PGC-1α

D, PPARα

E, PPARγ

F

G
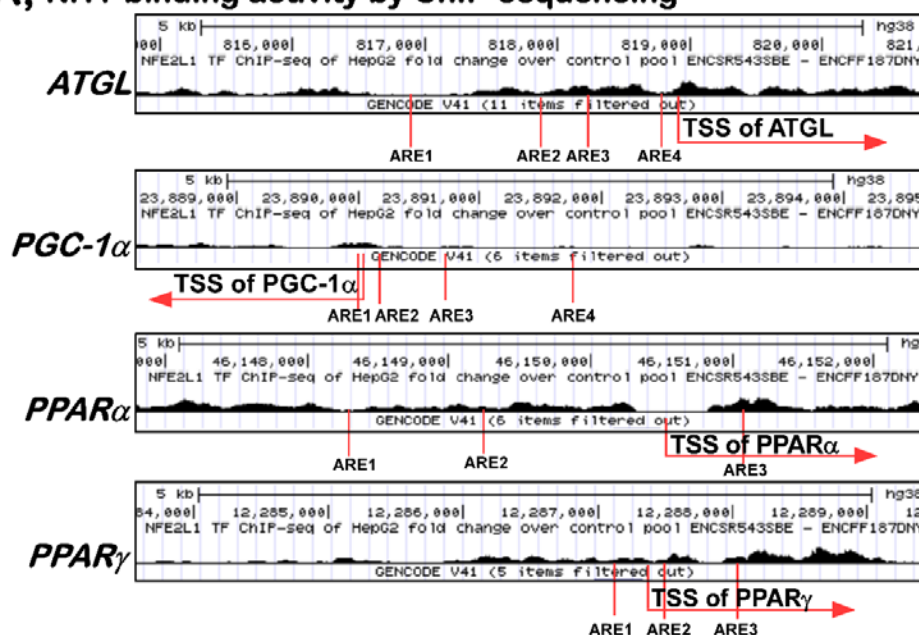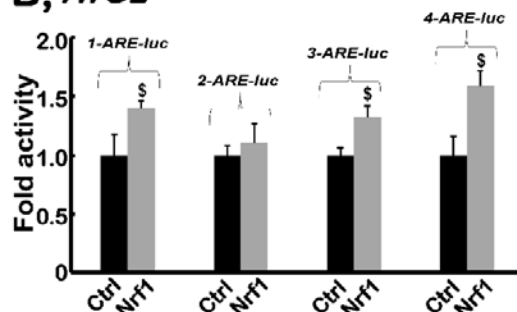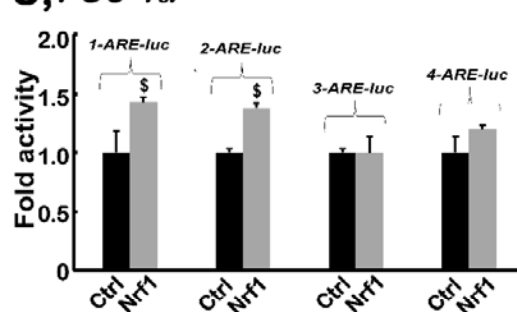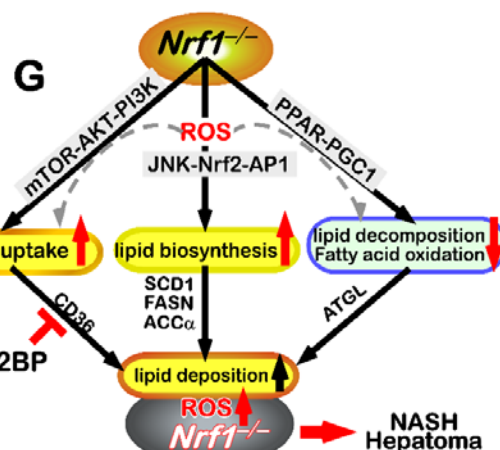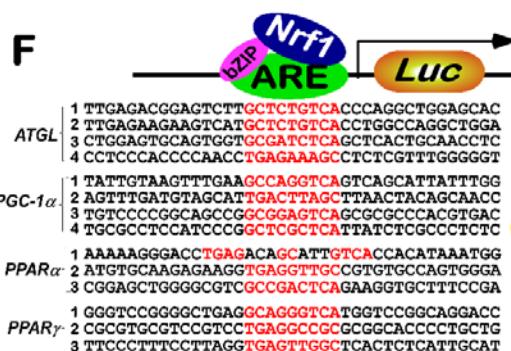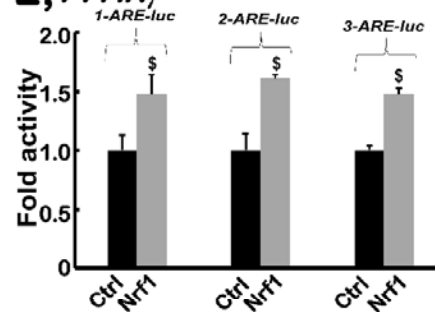
603 **Figure 6. Nrf1 mediates activation of *ARE*-driven luciferase reporters, along with a proposed model to explain the**
604 **molecular mechanisms underlying the inflammatory accumulation of lipids and ROS.** (A) The ChIP-sequencing date of Nrf1
605 (i.e., Nfe2l1, obtained from the Encode database) in the promoter regions of *ATGL, PGC-1α, PPARα* and *PPARγ* (the details of
606 which were also deciphered in supplemental Figure S3). The transcription starting sites and multiple *ARE* sites in the gene
607 promoter regions are marked. (B to E) *Nrf1/2$^{+/+}$* HepaG2 cells were co-transfected with each of those indicated *ARE-Luc* or
608 non-*ARE-Luc* (used as a background control) reporter plasmids, together with an expression construct for Nrf1 or an empty
609 pcDNA3 vector (serves as an internal control). Then luciferase activity was normalized to their internal p-*RT* reporter controls
610 and also corresponding backgrounds obtained from co-transfection with non-*ARE* reporter and each of the indicated
611 expression constructs. The data were calculated as a fold change relative to the basal activity (at a given value of 1.0)
612 obtained from the transfection of cells with the empty pcDNA3 control and each *ARE*-driven luciferase plasmid. All the data
613 shown herein are representative of at least three independent experiments undertaken on separate occasions that were
614 each performed in triplicates. Significant differences in *ARE*-driven transactivation by Nrf1 were subjected to statistical
615 analysis by using the Student's *t*-test or MANOVA; significant increases ($, $p < 0.01$) were shown, by comparison to their
616 basal levels. (F) Fourteen of the indicated ARE-adjoining sequences from lipid catabolism related gene promoters were
617 inserted into the pGL3-Promoter vector to give rise to *ARE-Luc* reporter genes. (G) A model was proposed for the molecular
618 mechanisms underlying the inflammatory accumulation of lipids and ROS in *Nrf1α$^{-/-}$* cells. This schematic provides an
619 overview of the molecular mechanisms by which the inflammatory accumulation of lipids and ROS occurs in *Nrf1α$^{-/-}$* cells.
620 Notably, *Nrf1α$^{-/-}$* cell-autonomous induction of the PI3K-AKT-mTOR signaling to up-regulation of CD36 results in augmented
621 uptake of fatty acids. The *de novo* biosynthesis of lipids is up-regulated by the JNK-Nrf2-AP1 signaling to transactivation of
622 their target genes encoding those key metabolic rate-limiting enzymes and their transcription factors, while the lipid
623 oxidative decomposition pathway is down-regulated by the PPAR-PGC1 signaling cascades. Altogether, these result in the
624 inflammatory accumulation of lipids and ROS in *Nrf1α$^{-/-}$* cells, but this pathological process is alleviated substantially by
625 2-bromopalmitate (2BP) to down-regulate the expression of CD36 regulated by Nrf1α.
626
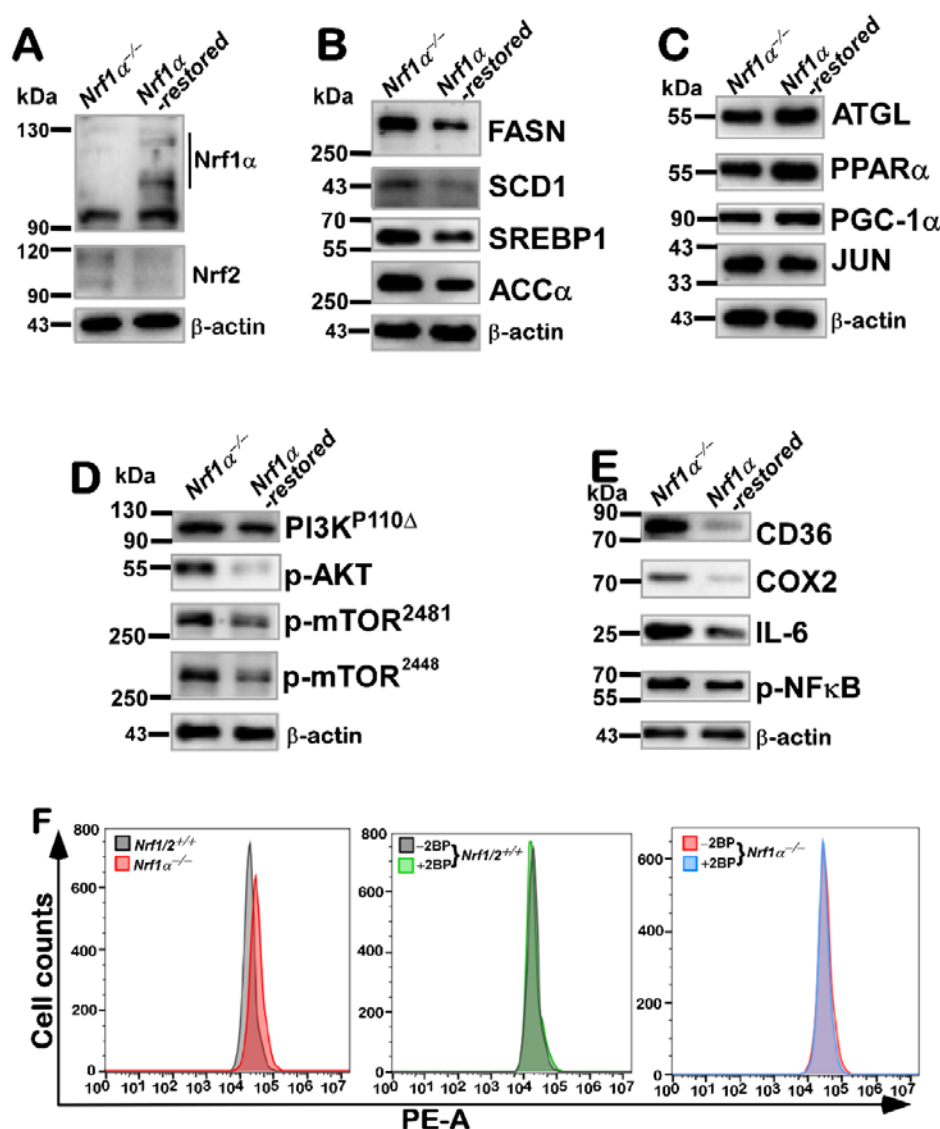627 **Supplemental Figure legends**

628

Figure S1
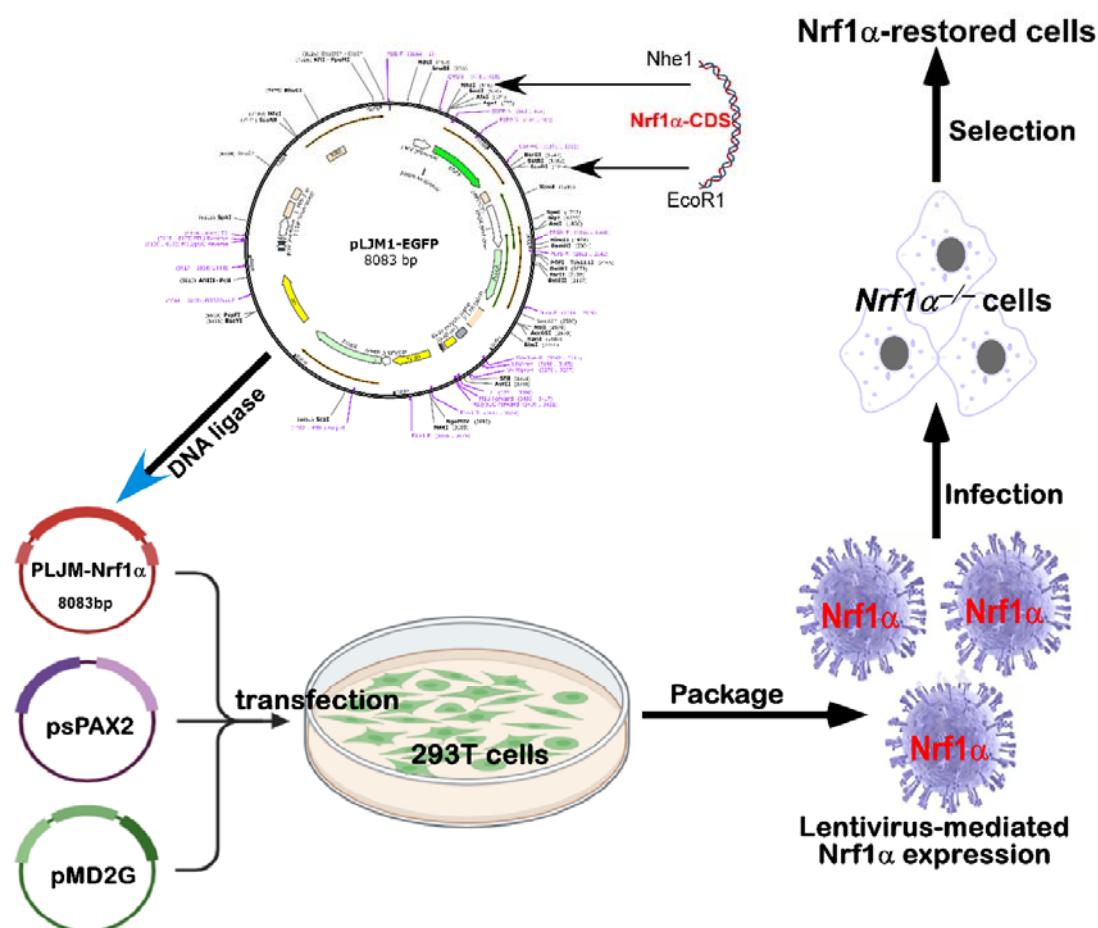
629 **Figure S1.** A flow chart for a lentivirus-packaged pLJM1-Nrf1α plasmid that was constructed and then infected into HepG2
630 cells, before a monoclonal Nrf1α-restored expression cell line was established to allow for stable expression of ectopic Nrf1α.

631

Figure S2. A series of repeatable experiments using the Nrf1α-restored expression cell line, **in order to** confirm that those changes observed in *Nrf1α*^{−/−} cells could be rescued by restoring stable expression of Nrf1, so that accumulation of lipids and ROS, along with the inflammatory response in *Nrf1α*^{−/−} cells are substantially alleviated by 2BP. The expression levels of those examined proteins in the lentivirally-mediated recombinant Nrf1α-Restored cell lines were detected by Western blotting with indicated antibodies (A to E); Flow cytometry determination of ROS in *Nrf1/2*[+/+] and *Nrf1α*^{−/−} cell lines that had been treated

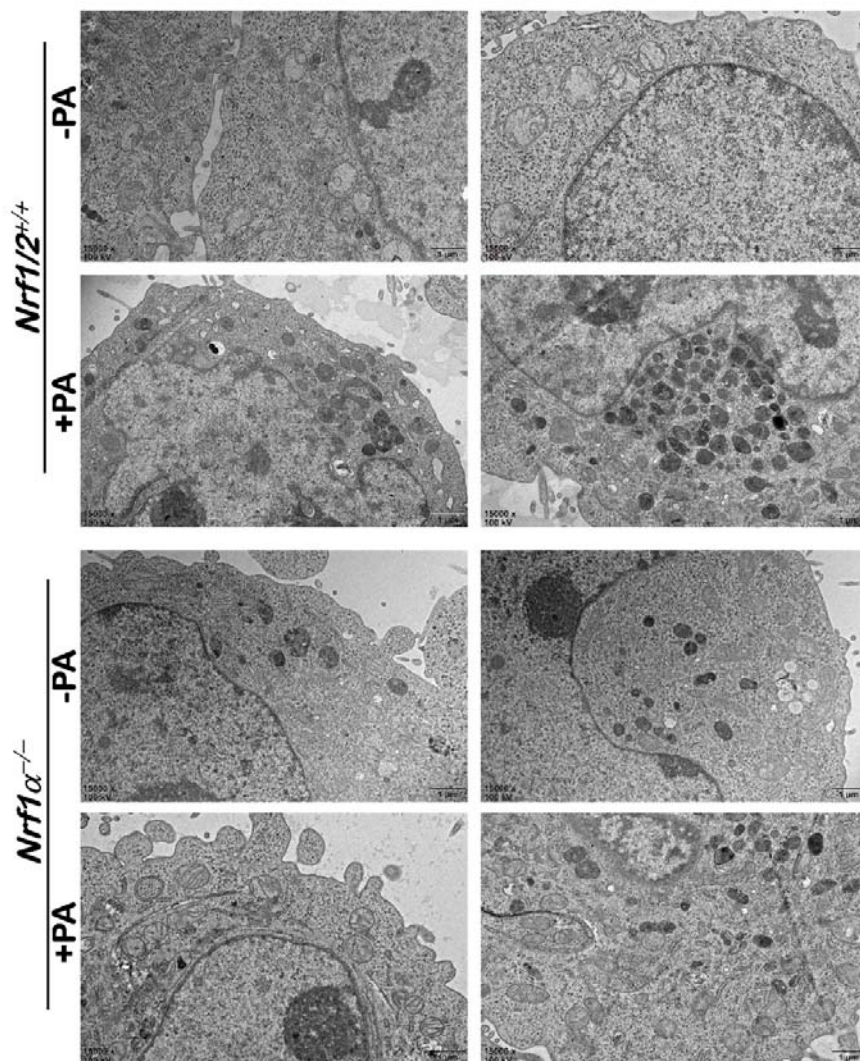637   with 2BP or without this this palmitic acid analogue, as described in the section of "Materials and Methods".

Figure S3

638
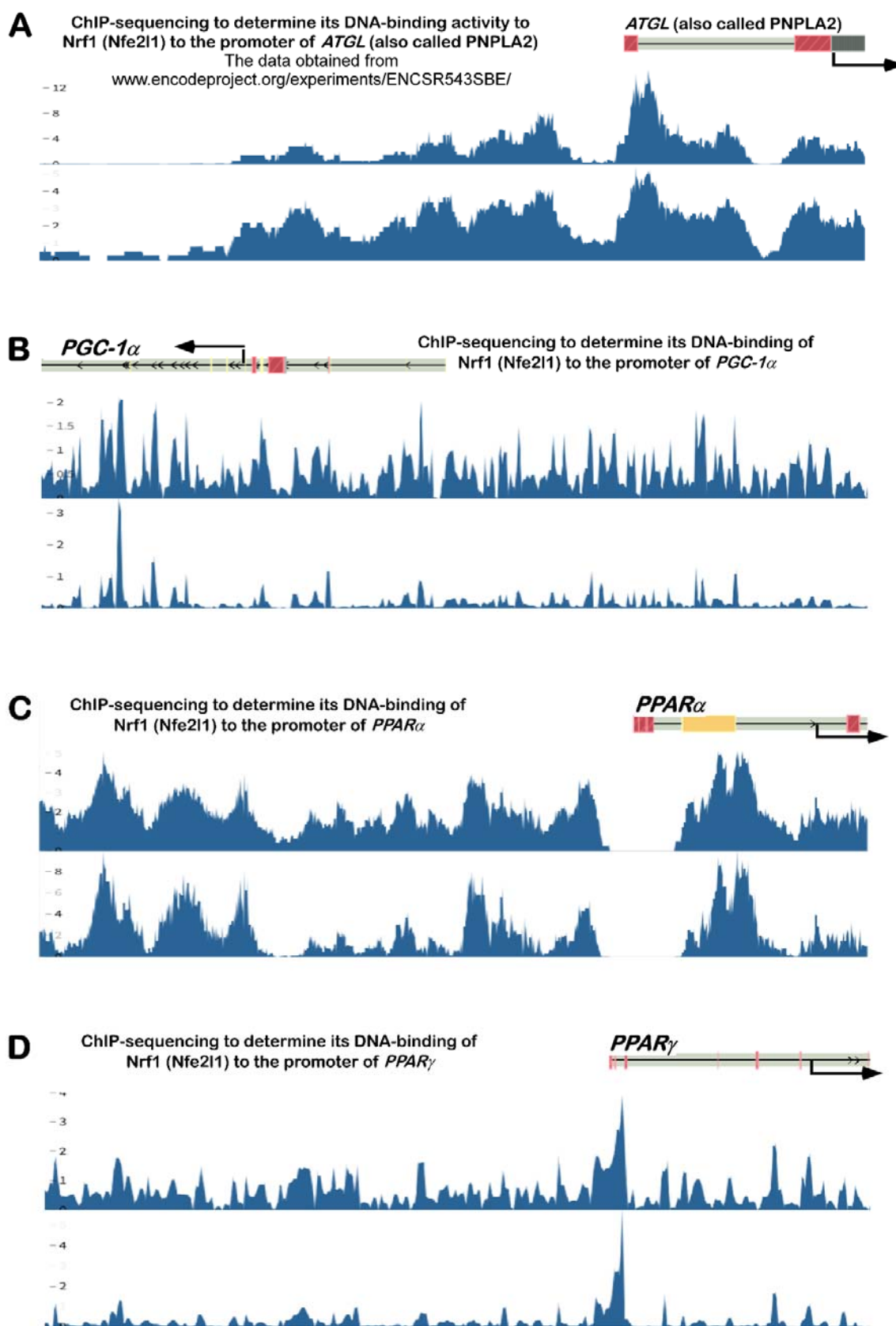
639   **Figure S3.** The ChIP-sequencing date of Nrf1 (i.e., Nfe2l1, obtained from the Encode database) binding to the promoter

640   regions of *ATGL, PGC-1α, PPARα* and *PPARγ*.

641

Figure S4

642   **Figure S4.** The electronic micrographs representing *WT* (*Nrf1/2$^{+/+}$*) and *Nrf1α$^{-/-}$* cell line that had been treated with palmitic

643   acids. The scale bar = 2 μm in ×2K pictures, or = 1 μm in ×7K pictures, or = 0.25 μm in ×20K pictures.